Advances in Rotorcraft Crashworthiness – Trends Leading to Improved Survivability

Karen E. Jackson, Ph.D.
Structural Dynamics Branch
NASA Langley Research Center
Hampton, VA 23681

NOMENCLATURE

List of Symbols

° - unit of angle, degree(s)
ft – unit of length, foot or feet
g – acceleration relative to the acceleration of gravity
Hz – unit of frequency, Hertz
in – unit of length, inch
lb – unit of weight or force, pound
mm – unit of length, millimeter
s – unit of time, second

List of Acronyms

AATD – Aviation Applied Technology Directorate
AC – Advisory Circular
ACAP – Advanced Composite Airframe Program
ACSDG – Aircraft Crash Survival Design Guide
ADS – Aeronautical Design Standard
AH – Attack Helicopter
AHSI – American Helicopter Society International
ALE – Arbitrary Lagrange-Euler
ARAC – Aviation Rulemaking Advisory Committee
ATB - Articulated Total Body
ATD – Anthropomorphic Test Device
CAL3D - Cornell Aeronautics Laboratory Three Dimensional
CIRA – Italian Aerospace Research Center
CFR – Code of Federal Regulations
CH – Cargo Helicopter
CRC-ACS - Cooperative Research Centre for Advanced Composite Structures
DAS – Data Acquisition System
DEA – Deployable Energy Absorber
DLR – German Aerospace Center
DOD – Department of Defense
EFG – Element Free Galerkin
FAA – Federal Aviation Administration
FM – Frequency Modulated
FSC – Full Spectrum Crashworthiness

GHBMC – Global Human Body Model Consortium
HIB – Hydro Impact Basin
HSTM – Human Surrogate Torso Model
HTFEM – Human Torso Finite Element Model
IDRF – Impact Dynamics Research Facility
JHU-APL – Johns Hopkins University – Applied Physics Laboratory
LandIR – Landing and Impact Research
LEM – Lunar Excursion Module
LISA - Aerospace Structures Impact Test Facility
LLRF – Lunar Landing Research Facility
LSTC - Livermore Software Technology Corporation
MADYMO - MAterial DYnamic Model
MIL-STD – Military Standard
NASA – National Aeronautics and Space Administration
PC – Personal Computer
RAH – Reconnaissance and Attack Helicopter
SAE – Society of Automotive Engineering
SARAP – Survivable Affordable Reparable Airframe Program
SMP - Symmetric Multi-Processing
SOM-LA – Seat/Occupant Model-Light Aircraft
SOM-TA – Seat/Occupant Model-Transport Aircraft
SPH – Smooth Particle Hydrodynamics
THOR – Test device for Human Occupant Response
THUMS – Total Human Model for Safety
TRACT – Transport Rotorcraft Airframe Crash Testbed
TVA – Technology Validation Article
UH – Utility Helicopter
US – United States
VPV – Virtual Prototype and Validation
VTA – Vertical Test Apparatus
WIAMAN – Warrior Injury Assessment MANikin
YPG - Yuma Proving Ground

ABSTRACT

This paper documents progress in rotorcraft crashworthiness research and development that has been realized during the past forty years. Trends are presented in several categories including: facilities and equipment for conducting crash testing, updated crash certification requirements, the application of crash modeling and simulation techniques, and rotorcraft structural design for improved crash performance focusing on the application of advanced composite materials. Likely one of the most important advances is the ability to rapidly simulate crash impacts and to see the effects of design changes on the impact response. Enhanced dynamic computer simulations have greatly improved automotive safety today and are making inroads in the aerospace community. Consequently, a detailed discussion of advances in crash modeling and simulation is presented. The paper concludes with a list of suggested recommendations, such that the progress made to date can be continued into the future.

INTRODUCTION

This paper addresses the topic of advancements and trends in rotorcraft crashworthiness. As part of the overall aircraft/rotorcraft design process, the incorporation of crashworthy features has become more important in today's environment, partly due to increased demands for improved safety by the flying public and partly due to new regulatory requirements. These features, such as energy absorbing subfloors, load-limiting seats, and active restraint systems, are intended to limit transient dynamic loads transmitted to the occupants during a crash event to survivable and/or non-injurious levels and to provide a livable volume that surrounds and protects the occupants. Additional crash-related design features include fire prevention, cabin delethalization, emergency lighting systems, mass retention, and post-crash egress.

As stated in Reference 1 "the optimal crashworthy design of an aircraft/rotorcraft utilizes a *systems approach* to provide the maximum level of protection for the occupants. Using this approach, the designer ensures that all of the separate safety systems in the aircraft work together to absorb the aircraft's kinetic energy and to decelerate the occupants to rest without causing injurious loading." An example of the systems approach is depicted in Figure 1, which highlights the three main contributors to energy absorption in a rotary-wing aircraft. Landing gear absorb energy to reduce the impact velocity of the fuselage, either through crash attenuating shock struts or permanent deformation of a skid gear. The subfloor structure provides additional deceleration through stable crushing and plastic deformation. The seat completes the system by limiting high deceleration loads that could be transmitted to the occupant. The seat must also remain attached to the floor to prevent the occupant from becoming a projectile within the cabin. The restraints must function well during the primary and secondary impacts to minimize head strike potential and occupant flail. The floor should be designed as primary structure to transfer load effectively between the seat and the subfloor. Finally, the fuselage cabin must be sufficiently stiff and strong to prevent intrusion of the overhead rotor transmission mass, which is a feature identified as mass retention.

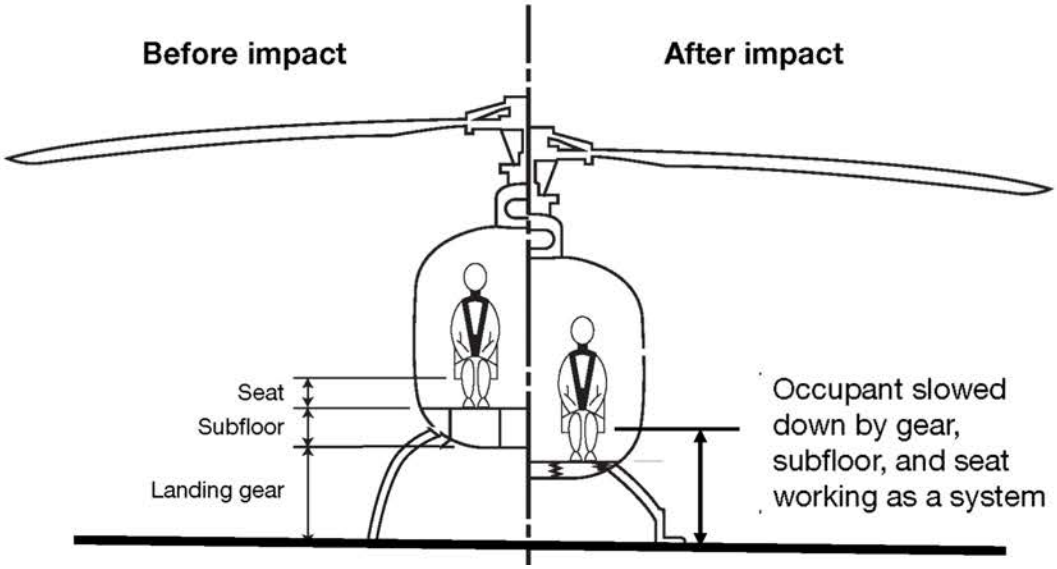

Figure 1. Schematic illustrating a systems approach to crashworthy design.

The crash performance of military helicopters has increased substantially over time. For example, a Department of Defense (DOD) sponsored study on rotorcraft survivability was provided to the United States (US) Congress in 2009 [2]. This study showed that for Cargo Helicopters (CH) and Utility Helicopters (UH), the loss rate during combat hostile action was nearly six times lower, and the fatality rate was four times lower, for Operation Enduring Freedom/Operation Iraqi Freedom versus the Vietnam War. This study noted that a high percentage of helicopter crashes are survivable and recommended that "to reduce personnel injuries and fatalities for combat threat losses and mishaps, improve airframe crashworthiness and crash protection for passengers. DOD crashworthiness standards have not been updated since the 1970's and need to be expanded in scope to cover a wider set of aircraft and environmental conditions."

Likewise, in 2009, the US Navy sponsored a study of Navy and Marine Corps helicopter accidents from 1985 to 2005 [3]. Conclusions from this study included: (1) The fatality rate per 100,000 flight hours reduced from 5.8 to 3.15, and the injury rate per 100,000 flight hours reduced from 3.92 to 2.14 between the first decade (1985-1994) and the second decade (1995-2005); (2) Decadal differences are attributed to improved policies, guidelines, training procedures and equipment; (3) Head injuries are an important cause of morbidity in helicopter mishaps; and (4) Non-pilot personnel appear to be at greater risk for injury.

In response to the 2009 Army report recommendation, the US Army Aviation Applied Technology Directorate (AATD) at Ft. Eustis, Virginia, sponsored an accident study as part of the Full Spectrum Crashworthiness (FSC) Program [4]. Findings of this study included: (1) crashworthy fuel systems have virtually eliminated fatalities and severe injures due to post-crash fire; (2) onboard systems such as lap belts, shoulder restraints, inertia reels, and load-limiting seats are effective in improving crash performance; (3) less than 20% of all mishaps studied occur onto rigid, prepared surfaces; and (4) the 90^{th}-percentile survivable impact ground speeds and vertical speeds for aircraft designed to

crashworthy criteria were generally higher than those for the previous generation of aircraft. For example, the Attack Helicopter (AH-64) Apache helicopter exceeded the AH-1 Cobra helicopter in both ground speed and vertical speed for both direct-to-terrain crashes and post-obstacle crashes. Likewise, the UH-60 Black Hawk exceeded the comparable speeds for the UH-1 Huey helicopter. Note that the AH-64 Apache and the UH-60 Black Hawk helicopters were designed to meet crashworthiness certification requirements, whereas the AH-1 Cobra and the UH-1 Huey were not.

Civilian helicopter accident survivability has shown improvement, as indicated in Table 1. Table 1 documents data, released by the Federal Aviation Administration (FAA), on the US helicopter accident rate and the fatal helicopter accident rate for the past 4 years, 2013-2016 [5]. Both rates have fallen for the third consecutive year. The accident rate is calculated per 100,000 flight hours. The FAA notes that, though there is only a very slight decrease in the fatal accident rate from 2015 to 2016, this rate is down significantly, almost 43%, since 2013. Overall, there has been a 27% decrease in the number of accidents when compared to 2013 [5]. Additional information on civilian helicopter accident statistics is documented in Reference 6. Interestingly, the improved numbers are attributed to collaboration between the FAA and the helicopter industry to better educate the civilian helicopter community on safe practices. In addition, the FAA and industry also are taking an active role in advancing safety through new technology, collaborative policy changes, and proactive outreach.

Table 1. Civilian helicopter accident statistics per 100,000 flight hours (Reference 5).

Year	Total Accidents	Total Accident Rate	Fatal Accidents	Fatal Accident Rate
2016	106	3.19	17	0.51
2015	121	3.67	17	0.52
2014	138	4.26	21	0.65
2013	146	4.95	30	1.02

The trends reported in References 2-6 are encouraging and they represent advancements made in rotorcraft crashworthiness over the past forty years to the present time. The objectives of this paper are to examine the contributions to this improvement from four specific technical areas: facilities and equipment for conducting crash testing, updated crash certification requirements, the application of crash modeling and simulation techniques, and rotorcraft structural design. The objectives of this paper are to assess past technology, to examine the state-of-the-art, and to make recommendations for the future.

FACILITIES AND EQUIPMENT FOR CONDUCTING CRASH TESTING

This section of the paper describes full-scale crash test facilities and vertical drop towers used for conducting crash and/or vertical impact tests of full-scale aircraft/rotorcraft. In addition, equipment

used to support full-scale testing, such as data acquisition systems, photogrammetry, anthropomorphic test devices, and cameras, are also discussed.

Full-Scale Crash Test Facilities

Landing and Impact Research (LandIR) Facility, Hampton, VA

During the Apollo program, the National Aeronautics and Space Administration (NASA) constructed a large gantry, designated the Lunar Landing Research Facility (LLRF), to allow astronauts to practice the last 150-ft of descent onto a simulated lunar surface under recreated $1/6^{th}$ gravitational conditions of the Moon. As shown in Figure 2(a), the LLRF is a steel A-frame structure that is 240-ft tall, 400-ft in length, and 265-ft wide at the base. The surface beneath the gantry was cratered to look like the surface of the moon. The Apollo astronauts practiced simulated lunar landings in the Lunar Excursion Module (LEM), one of which is shown in Figure 2(b). In 1985, the facility was designated a National Historic Landmark based on its significant contributions to the Apollo Moon Landing Program. References 7 and 8 describe the operational features of the LLRF and the results of tests performed using the facility.

(a) Photograph of the LLRF. (b) Photo of the Lunar Excursion Module (LEM).

Figure 2. Photographs depicting the Lunar Landing Research Facility (LLRF) and the Lunar Excursion Model (LEM), which is suspended from the gantry.

At the end of the Apollo program, the LLRF was converted into a full-scale test facility for investigating the crashworthiness of light aircraft/rotorcraft and was designated the Impact Dynamics Research Facility (IDRF) [9]. A photograph of the gantry structure is shown in Figure 3(a). The purpose and benefit of full-scale crash testing, as defined in Reference 9, is "to obtain definitive data on the structural response of aircraft and on the loads transmitted to the occupants during a crash impact. These data can be used for correlation with results of analytical predictive methods. Full-scale aircraft crash tests can also be used to evaluate crashworthy design concepts both for the aircraft structure and for seats and restraint systems." One of the important features of this facility is the ability to perform full-scale crash tests of light aircraft and rotorcraft under free-flight conditions;

and, at the same time, to control the impact attitude and velocity of the test article upon impact. Full-scale crash tests can be performed for a wide range of combined forward and vertical velocity conditions. Details of past crash test programs conducted at the IDRF are documented in References 10 and 11.

In 1981, a 70-ft vertical drop tower, designated the Vertical Test Apparatus (VTA), was connected to the northwest leg of the gantry for the purpose of conducting vertical drop tests. A picture of this addition is shown in Figure 3(b). In 2000, the lifting capacity of the pull-back bridge was increased to its current level of 64,000 lb. In 2006, the gantry facility underwent a name change from IDRF to Landing and Impact Research (LandIR) facility in recognition of the fact that the focus of testing had changed to include spacecraft landing, as well as aircraft crash testing. In addition, a Hydro Impact Basin (HIB) was constructed on the western end of the facility for the purpose of conducting impact tests into water. Construction began in June 2010 and was completed in March 2011. The HIB is 115-ft long, 90-ft wide, and 20-ft deep. A photograph of the LandIR facility is shown in Figure 4 with the HIB and the 70-ft VTA highlighted. During the past six years, the HIB has been used to conduct 47 combined and vertical velocity impact tests of the Orion space capsule as well as other test articles. With the addition of the HIB, the LandIR facility is now capable of multi-terrain impacts onto soft soil, rigid surface, and water.

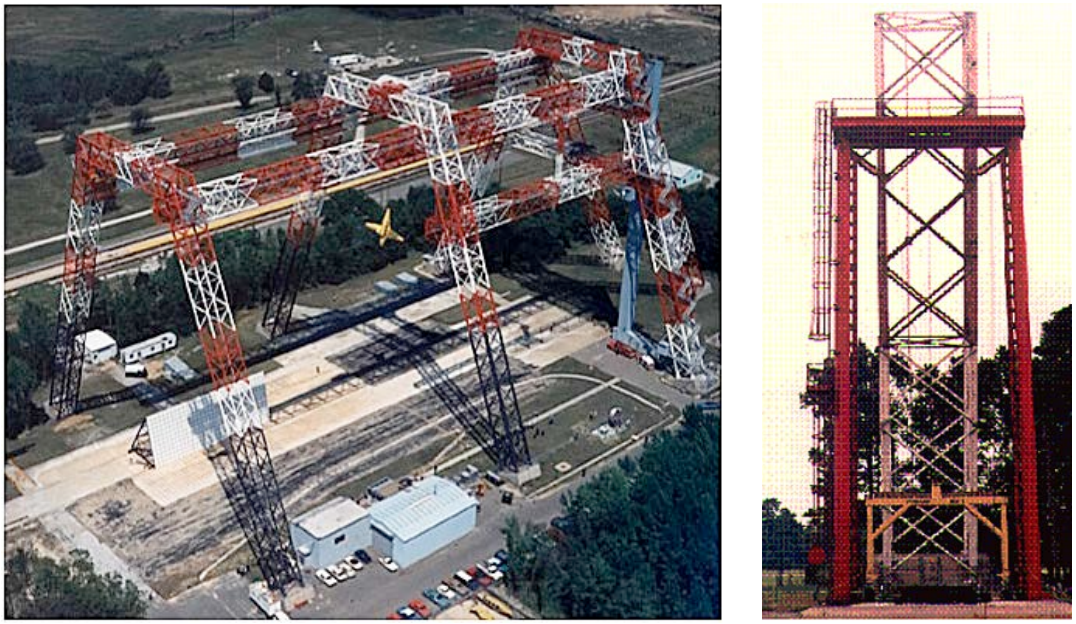

(a) Impact Dynamics Research Facility (IDRF). (b) Vertical Test Apparatus (VTA).

Figure 3. Photographs of the IDRF and the VTA.

Crash tests performed at the IDRF used a pendulum-swing technique. Two swing cables are attached from the western top end of the gantry to the test article. A pull-back cable is suspended from the loading bridge, which transverses the gantry, to the test article through a winch system. The test article is raised to the drop height by shortening the pull-back cable using the winch. Following a countdown, the pull-back cable is released allowing the test article to swing towards the impact

surface. All supporting cables are pyrotechnically cut at a short distance above the impact surface, allowing the test article to impact the surface in free-flight conditions. This test approach has worked well and introduces combined forward and vertical velocities at impact of the test article. Unfortunately, this test approach also introduces a pitch angular velocity, which is often not desireable. For example, if the purpose of the test is to collect data for model calibration, then the precise impact conditions must be determined including initial angular velocities, which can be difficult to measure.

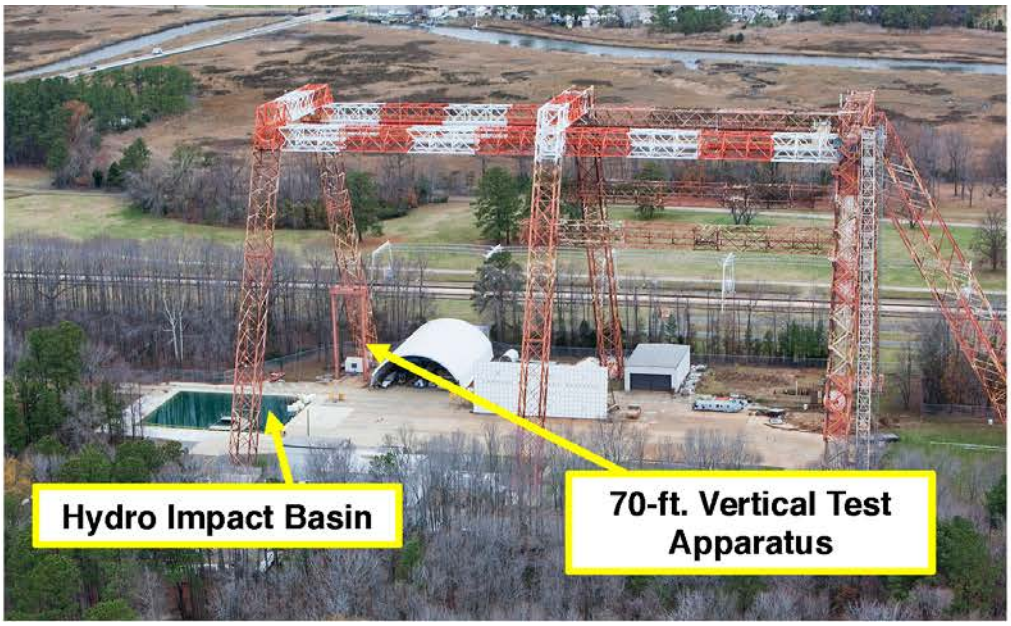

Figure 4. Photograph of the LandIR facility.

A new approach for performing full-scale impact tests was developed based on a parallelogram arrangement of the swing cables and an integration platform. This approach is illustrated in Figure 5 in which the test vehicle is an Orion Boilerplate Test Article. Using this approach, two sets of swing cables (two cables per set), of the same length, are attached to the integration platform in a parallelogram configuration. Two pull-back cables are also attached. During the test, the pull-back cables are used to raise the test article/integration platform to the correct drop height. Following a countdown, the pull-back cables are cut, allowing the test article/integration platform to swing towards the impact surface. Because of the parallelogram arrangement of the swing cables, the test article does not develop a pitch angular velocity. At a designated height above the impact surface, the cables connecting the test article to the integration platform are severed allowing the test article to hit the impact surface with the required forward and vertical velocities. The integration platform continues to swing following release of the test article.

LISA Crash Test Facility, Capua, Italy

The largest crash facility in Europe, known as LISA Aerospace Structures Impact Test Facility, was built by CIRA, the Italian Aerospace Research Center. The facility was officially opened on April 8, 2002 in Capua, Italy. The LISA facility is used to perform research applicable to aeronautical and

space applications including: (1) Numerical and experimental analyses, demonstrations, certification and qualification of aircraft subjected to catastrophic impact; (2) Analysis and experimentation of high-energy crash impacts on ground and water surfaces; (3) Numerical and experimental analyses, demonstrations, certification and qualification of aircraft subjected to ditching; (4) Support provided to aerospace industries during design and/or qualification/certification of structures subject to high-energy impacts; and (5) Support given to aeronautical certification agencies on crashworthiness issues.

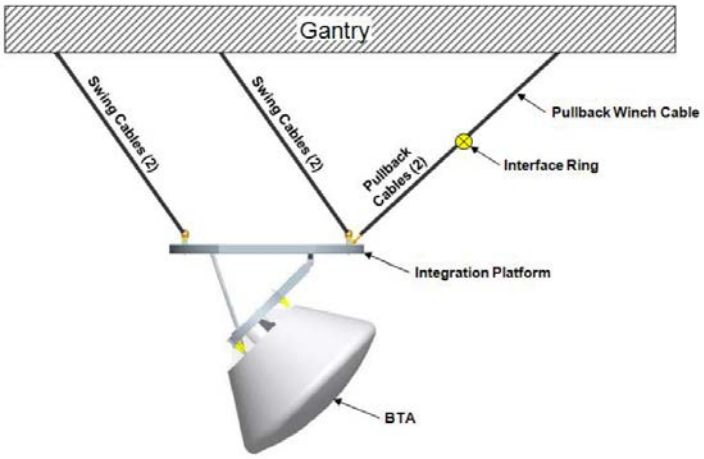

Figure 5. Integration platform and parallelogram test method schematic.

LISA includes two main facilities: an impact test facility for full-scale aerospace structures and a ditching/emergency landing test facility. The facility provides a controlled impact speed and angle for aircraft weighing up to 44,000 lbs. The aircraft can be tested onto a rigid surface, soft soil, or water. In the future, the water pool will be equipped with a wave generation system for ditching studies. A photograph of the LISA facility is shown in Figure 6. The LISA facility has been dormant for the past seven years.

Figure 6. Photograph of the LISA Aerospace Structures Impact Test Facility.

Water Impact Test Facility

In the late 1990's, the Navy awarded a Small Business Innovative Research contract to Dynamic Response Incorporated, Simula Technologies, Inc., and Bell Helicopter to study water impact [12]. Simula entered into a cooperative agreement with the US Army Yuma Proving Ground (YPG) with the objective to develop and demonstrate a water impact dynamic test facility for aircraft. The test facilities and methodologies have since been utilized for several water and soft-soil impact tests. Vertical drop tests of a UH-1 Huey helicopter were performed by lifting the aircraft with a crane to a pre-determined height, positioning it over the drop zone, and releasing it. For water impact tests, the drop zone was the ground vehicle fording basin at YPG.

Impact tests that required combined vertical and forward velocity components are more difficult and required a much more complicated test-set. The main problems are controlling the attitude of the test article at impact, and releasing the test article at the precise moment. The test procedure developed during this program solved the impact attitude and release problem through the use of a trolley-and-guide-beam system. As depicted in Figure 7, the guide trolley is rigidly connected to the helicopter at the rotor mast mount. Upon initial release, the helicopter accelerates down the guide beam on the flight path dictated by the beam's angle, and at the attitude held fixed by the guide trolley. At the end of the beam run, the trolley simply "falls off" of the end of the beam, allowing the test vehicle to impact the water. The guide trolley is located and ballasted to provide the same inertial properties as the rotor transmission mass. The current status of this facility is unknown.

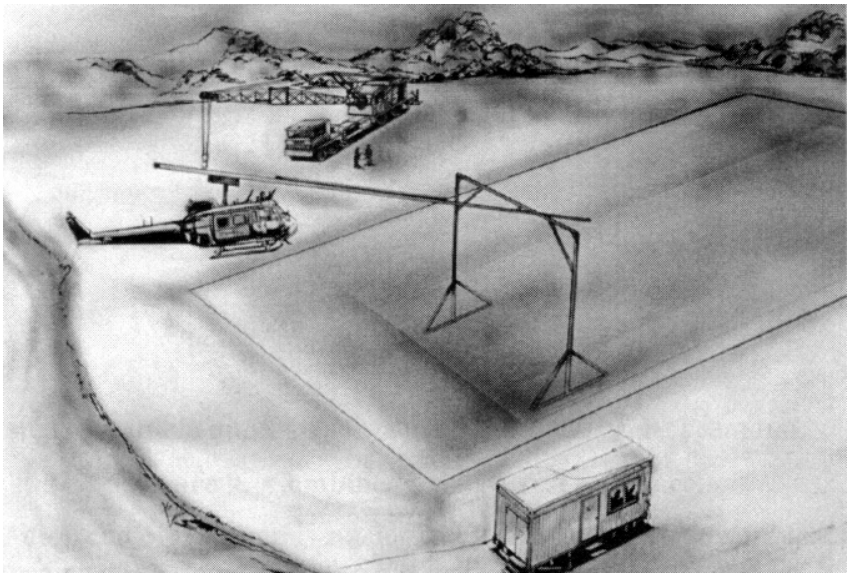

Figure 7. Schematic of the Water Impact Test Facility.

Vertical Drop Towers

In addition to the VTA at LandIR, a Dynamic Drop Test Facility is located at the FAA William J. Hughes Technical Center in Atlantic City, New Jersey, and has been used to perform vertical drop

tests of aircraft and fuselage sections, as shown in Figure 8. Aircraft or fuselage components are suspended from the 57-ft-high tower and released to fall unrestrained onto either a wooden platform or a concrete surface. Currently, this facility is mothballed. Other vertical drop test facilities are located at the US Army Aberdeen Proving Ground, the US Army Aeromedical Research Laboratory, the US Air Force Wright-Patterson Research Laboratory, US Naval Air Systems Command, and the National Institute of Aviation Research at Wichita State University. These facilities have a range of lifting capabilities and drop heights and may only be capable of conducting aircraft component drop tests, as opposed to drop tests of full-scale aircraft.

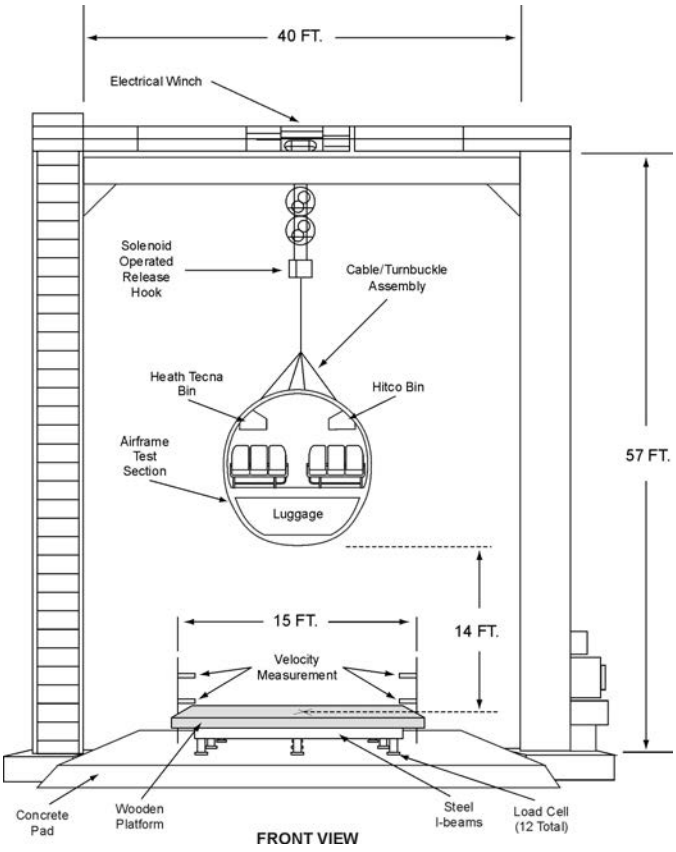

Figure 8. FAA Dynamic Drop Test Facility.

Equipment

Data Acquisition Systems

Crash testing is only as successful as the data collected during the test. Tremendous improvements in Data Acquisition Systems (DAS) have enabled the collection of hundreds of channels of data during a test. At the IDRF, the original data collection system utilized Frequency Modulated (FM) multiplexed analog tape recorders. Electronic data from transducers on the test article were transmitted over a large umbilical cable that ran from the test article, to the top of the gantry, and into the instrumentation room. Data were collected on analog tapes, which were sent out for data reduction and analysis following a test. Several days later, printouts of engineering data plots and digital ascii data were made available. Using the analog system, a maximum of 96 channels of data could be recorded at 4,000 samples per second per channel [13]. In the mid-to-late 1990's, the analog system

was replaced with a ruggedized, onboard digital DAS, capable of recording up to 512 channels of data from instruments including accelerometers, strain gages, rate sensors, and lumbar load cells, at a maximum rate of 100,000 samples per second per channel. Following a test, the data are downloaded to a computer and can be viewed almost instantaneously. Thus, the digital DAS represents a quantum leap in improvement over the analog system.

Photogrammetry

One relatively new capability for data collection at LandIR is large field photogrammetry [14, 15]. As an example of this technology, a CH-46E Sea Knight helicopter is depicted in Figure 9 in which 1-in.-diameter black dots were painted in a random pattern on one side of the airframe. This helicopter was crash tested at the LandIR facility in 2014 as part of the Transport Rotorcraft Airframe Crash Testbed (TRACT) program [16]. During the crash test, the position of each dot was tracked in time using 3-dimensional photogrammetry. The recorded data are then used to create, for example, fringe plots of lateral displacement, as shown in Figure 10. The lateral deformations are clearly visible just at window height, indicating dilation of the airframe as the bottom of the helicopter impacts the soil during the test. This capability provides important information regarding airframe deformations and motion and is a welcome addition to the LandIR facility.

Figure 9. Dot pattern shown on a CH-46E helicopter.

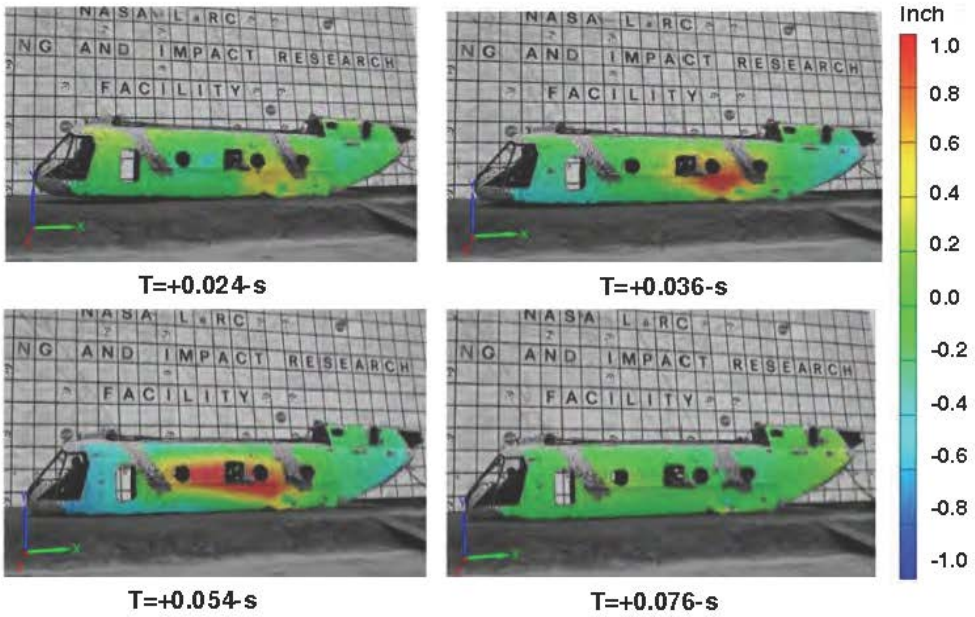

Figure 10. Impact sequence of lateral displacement obtained from photogrammetry.

Anthropomorphic Test Devices (ATDs)

A full-scale Anthropomorphic Test Device (ATD) is a crash test dummy that replicates the dimensions, weight proportions and articulation of the human body, and is usually instrumented to measure the dynamic behavior of a simulated human occupant during vehicle impacts. ATDs are widely used in the automotive industry to predict the biomechanics, impact forces, and potential injuries that might be experienced by a human occupant in an automobile crash. As documented in Reference 17, ATDs were initially developed in the late 1940's to evaluate ejection seats on rocket sled tests for the US Air Force. The first ATD, Sierra Sam, was a 95th percentile male dummy, developed by Sierra Engineering. The human-like characteristics of this dummy were based on US Air Force personnel anthropometry. This dummy had limited instrumentation capability (head accelerometers only), but was considered state-of-the-art at the time. By the mid-1960's, it became apparent that the ATDs developed specifically for aircraft ejection seats were inadequate for automotive use. These dummies had no pelvic structure and poor spinal fidelity. Ford Motors sponsored development of Sierra Stan, a 50th percentile male dummy, which was specifically designed to meet the needs of the automotive industry. In 1972, the Hybrid II 50th percentile adult male dummy was specified in Part 572 of the Code of Federal Regulations (CFR) to be used in automotive testing. While the instrumentation capability of this dummy was limited, it represented state-of-the-art in dummy technology in the early 1970's.

The Hybrid III ATD was released in 1976 as a 50th percentile male dummy [18]. Again, this dummy was specifically developed to be used in crash testing of automobiles, as indicated in CFR Part 572. The Hybrid III allowed additional instrumentation including head, chest and pelvic accelerometers, as well as chest displacement, and head/neck loads and moments. In 1987, small female (5th percentile) and large male (95th percentile) versions of the Hybrid III were developed. Development of the Test device for Human Occupant Restraint (THOR) dummy began at Humanetics Incorporated in 1985. The initial release of THOR came in 1995, with subsequent modifications and updates. The most recent version is THOR-K, which incorporates enhanced biofidelic features and significantly expanded instrumentation compared to the standard Hybrid III 50th percentile adult male ATD. Today, the cost of a THOR ATD is approximately $400,000.

Except for the early ATDs that were developed specifically for ejection seat testing, most of the later dummies were designed for automotive impact testing, with one exception. In 2006/2007, the US Army sponsored the development of a Warrior-representative test dummy with associated biomedically-validated injury assessment tools for use in live-fire testing and vehicle development efforts. A particular focus for Warrior Injury Assessment MANikin (WIAMAN) was the ability to predict human occupant responses to blast loading [19]. Thus, WIAMAN was designed to accurately respond to loading in a direction parallel to the spine; however, WIAMAN has never been used in a full-scale crash test of an aircraft/rotorcraft. A pictorial view highlighting the evolution of these dummies is shown in Figure 11. The LandIR facility currently has 10 ATDs including a 5th percentile Hybrid III female, a 95th percentile Hybrid III male, many Hybrid II 50th percentile male dummies, a 6-year-old child, and a 3-year-old child.

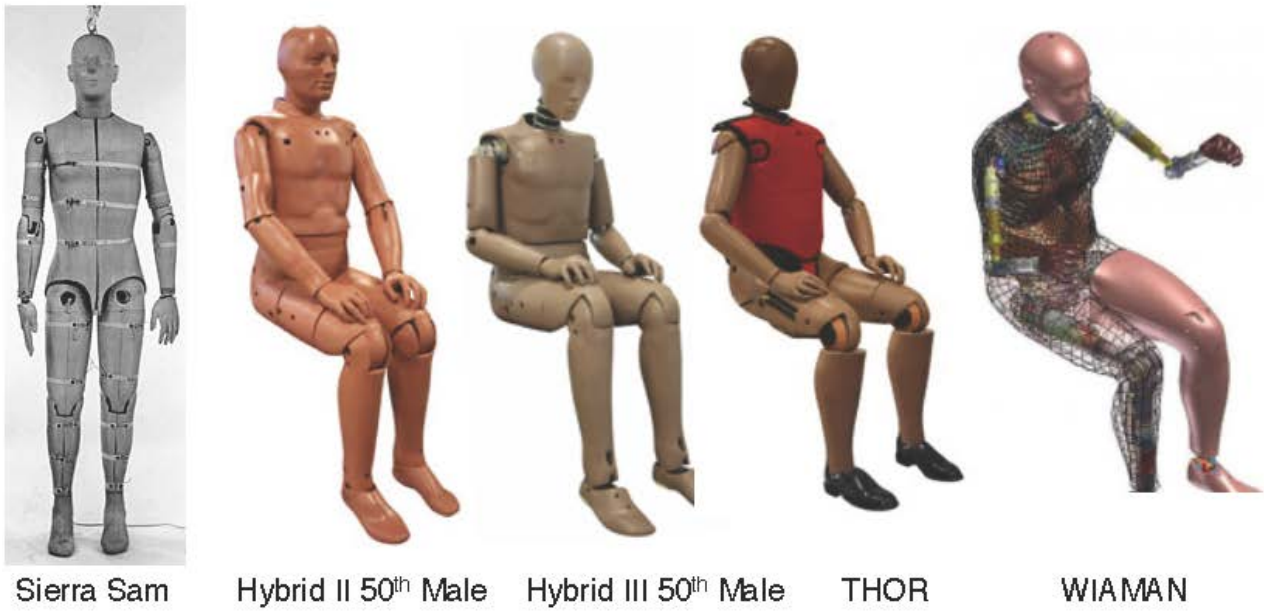

Figure 11. Depiction of the evolution of ATD test dummies.

High-Speed Cameras

Other important equipment needed in conducting a full-scale crash test are cameras to provide motion picture data. In the 1980's, Milliken 16-mm film cameras were used to capture test responses at 400 frames per second, both onboard and external to the test article. Following a test, films obtained during the test were sent out for processing, which required approximately one week of turnaround time. Currently, LandIR has a combination of different types of camera systems available, all of which collect digital images. Six high-speed cameras are used for capturing onboard images at 500-frames per second. Numerous point-of-view high-definition cameras are also used to collect onboard data. Twelve high-speed ground cameras are typically mounted on tripods and located around the exterior perimeter of the test article. These cameras record visual data at 1,000 frames per second. Two of the ground cameras are typically dedicated for photogrammetry. Finally, LandIR also has an underwater high-speed camera to collect data at 1,000 frames per second for tests using the HIB.

UPDATED CRASH CERTIFICATION REQUIREMENTS

Military helicopter design requirements for crashworthiness were developed by close examination of US Army accident data. Accident data were evaluated to determine velocity changes in the vertical and forward directions at impact for survivable crashes. The results showed that the 95th percentile of all survivable accidents occurred at less than 42.0-ft/s vertical and 50-ft/s forward impact velocity changes. Analysis of the data also showed similarity between rotary- and light fixed-wing aircraft. Consequently, the same criteria were used to qualify both types of military aircraft. Findings from the review of accident data and many additional investigations into the safety and survivability of Army helicopters led to the development of the Aircraft Crash Survival Design Guide (ACSDG) in 1965, which was a compilation of a series of reports on accident analyses, full-scale crash test data,

proposed design criteria, and prototype crashworthy systems. Since then, the ACSDG has been updated and expanded several times to encompass the increasing knowledge gained from continuing research in rotorcraft crashworthiness. Today, the latest edition of the ACSDG [20], consists of five volumes.

Information contained in the ACSDG was used in the development of Military Standard MIL-STD-1290A (AV) for Light Fixed and Rotary-Wing Aircraft Crash Resistance [21], which established minimum crash resistance criteria for implementation in the early stages of aircraft system design. The initial release of the standard was in January 1974, and it was subsequently revised in September 1988. In the late 1980's, an Aeronautical Design Standard ADS-36 for Rotary Wing Aircraft Crash Resistance [22] was developed specifically for qualifying the US Army's new Reconnaissance and Attack Helicopter (RAH-66), which eventually became the Comanche helicopter. The ADS-36 contains similar information as the MIL-STD-1290A (AV); however, some of the criteria were modified so that the RAH-66 would be designed with crash resistance equivalent to the existing UH-60 Black Hawk helicopter. Appendix A in MIL-STD-1290A (AV) lists the mandatory testing requirements for various aircraft components and subsystems including the fuel system, crew and troop seats, litter supports, landing gear, and flammability tests. Note that the military standard states that a full-scale crash test is desirable for demonstrating compliance. However, the recommendation is not mandatory and analytical models are acceptable.

In 2000, the US Army initiated development of a FSC design guide to establish crashworthiness criteria for implementation starting in the initial stages of system design for a wide range of rotorcraft classes, types, configurations, and operating conditions that continue over the life cycle of the rotorcraft system [23, 24]. The FSC criteria identify the key components that contribute to a system's crashworthiness and provide a quantitative measure of crashworthy performance. Currently, the FSC design criteria are part of the anticipated crashworthiness requirements for the Future Vertical Lift helicopter. However, at this time, no helicopters have been designed using the FSC criteria. Consequently, the effectiveness of the new approach cannot be judged, as yet.

It is important to note that there are no aircraft-level crashworthiness requirements for civilian rotorcraft, similar to MIL-STD-1290A (AV) or ADS-36. Instead, there are dynamic seat requirements described in the CFR Parts 27 and 29, for normal and transport civil rotorcraft [25, 26]. These criteria are summarized in the Society of Automotive Engineers (SAE) Standard [27], and comparisons of military and civilian requirements are presented in References 28 and 29. As with civilian helicopters, no aircraft-level crashworthiness certification requirements currently exist for General Aviation aircraft, regional jets, or transport aircraft. Instead, seat requirements are described in the CFR Parts 23 and 25 [30, 31]. However, it is useful to note that an Aviation Rulemaking Advisory Committee (ARAC) has been established to provide recommendations to the FAA regarding the incorporation of airframe-level crashworthiness and ditching standards into Title 14 CFR Part 25 for transport aircraft. The ARAC should complete its work and provide recommendations in 2018 [32].

CRASH MODELING AND SIMULATION

In the past forty years, significant advances have occurred in the development of explicit transient dynamic finite element codes for simulating the impact response of automotive and aviation vehicles during crash events. Commercial codes provide the ability to effectively evaluate structural designs analytically, thus reducing the need for full-scale crash testing. For the automotive and aircraft industries, use of finite element codes in designing crashworthy structures is proving to be a very cost effective approach. In addition, regulatory requirements have established the use of codes in the crashworthiness certification process. For example, in 2003 the FAA released an Advisory Circular (AC 20-146) providing guidelines for acceptable seat certification-by-analysis [33]. Recently, the FAA has proposed a revision to AC 20-146 on using certification-by-analysis for seating systems. In addition, MIL-STD-1290A (AV) contains seven different specifications for rotorcraft crashworthiness with associated performance requirements for each of the impact conditions. To meet the performance requirements, the designer is requested to demonstrate the capabilities of the aircraft to withstand various velocity change criteria using analytical methods. While the process of certification-by-analysis is gaining acceptance, continued efforts are needed to gain confidence in the capabilities of transient dynamic simulation methods, especially for structures fabricated of advanced composite materials [34].

As noted earlier, the military standard for crash resistance, MIL-STD-1290A (AV), clearly states the intent for the designer to demonstrate compliance with the various velocity change requirements through analytical methods. There were likely two reasons for encouraging the use of analytical methods. First, providing full-scale aircraft for destructive crash testing, especially prototype aircraft, can be expensive. Also, due to limited availability and the high cost of test articles, it is generally not feasible to perform repeated tests or a large number of tests for different impact conditions. Secondly, the timeframe for the initial publication of the military standard in the mid 1970's corresponded with the initial release of KRASH, a kinematic lumped-spring-mass crash analysis code [35, 36].

During this same time period, a new code, DYNA3D [37], was being developed at Lawrence Livermore National Laboratory under sponsorship by the Department of Energy. DYNA3D was an explicit transient dynamic finite element code capable of simulating high-speed impacts. Later, the public domain version of DYNA3D was obtained by commercial vendors who made modifications and now market commercial versions such as NASTRAN SOL 700 [38], PAM-CRASH [39] and LS-DYNA [40-42], to name a few of the spin-offs. To fully appreciate the progress made in the development of computational methods for crash analysis, it is important to understand changes in the state-of-the-art from the 1980's (KRASH) to the current time (LS-DYNA). As such, brief descriptions of KRASH and LS-DYNA are presented as well as examples of test-analysis comparisons for each simulation code.

KRASH

The Lockheed-California Company developed KRASH [35, 36] under initial sponsorship by the US Army in 1974. The FAA later supported further development of the code. The most recent public

domain version of the program to be released was KRASH85, and a commercial version was made available through Dynamic Response Incorporated, called DRI-KRASH. The KRASH program predicted the response of vehicles to multidirectional crash environments. Structural models were developed from massless interconnecting beam elements, concentrated rigid body masses, and spring elements. The beams represented the stiffness characteristics of the structure between the masses. Plastic deformation was accounted for through stiffness reductions. Concentrated masses translated and rotated under the influence of external forces including gravity and impact forces, as well as the constraint provided by internal element forces. Impact forces were introduced into the model through nonlinear external springs attached to the masses. In general, the development of KRASH kinematic models required considerable engineering judgment to define the beam stiffness properties. The models were small, consisting of only a few beam elements, masses, and springs. Consequently, they could be executed quickly on a Personal Computers (PC). KRASH simulations relied heavily on experimental data as input to define spring stiffness properties. For example, spring elements might be used to represent the crushing response of the subfloor/tub section or the crushable stage in a landing gear. Component crush test data were used to define the load-deflection response of the springs.

LS-DYNA

LS-DYNA [40-42] is a general-purpose finite element code for analyzing the large deformation, transient dynamic response of structures including structures coupled with fluids. LS-DYNA is a commercial code marketed by Livermore Software Technology Corporation (LSTC) and is widely used by the automotive and aerospace industries today. The main solution methodology is based on explicit time integration; however, an implicit solver is also available. A wide variety of contact definitions are available including self-contact, surface-to-surface contact, and node-to-surface contact. Spatial discretization is achieved by the use of eight-node solid elements, two-node beam elements, three- and four-node shell elements, truss elements, membrane elements, discrete elements, and rigid bodies. LS-DYNA currently contains over two hundred constitutive models and equations-of-state to cover a wide range of material behavior. Fluid-structure interaction problems are simulated using Arbitrary Lagrange-Euler (ALE) coupling. Smooth Particle Hydrodynamic (SPH) and Element Free Galerkin (EFG) methods were added to provide additional "hydrocode" capabilities. LS-DYNA is operational on mainframe computers, workstations, and PCs, and can be executed using shared memory processors, or with multiple parallel processors.

Illustrative Example of Test and Analysis Comparison: KRASH

Since KRASH was developed under sponsorship by the US Army and was initially released at approximately the same time as the military standard for crash resistance, it is appropriate to assume that the Army would encourage the use of this code by defense contractors in developing new aircraft and would accept KRASH simulation results as proof of crash performance. In the late 1970's, the US Army initiated the Advanced Composite Airframe Program (ACAP) [43-49]. The purpose of the ACAP was to demonstrate the potential of advanced composite materials to save weight and cost in airframe structures while achieving systems compatibility and meeting Army requirements for

vulnerability reduction, reliability, maintainability, and crash resistance. In 1981, the US Army awarded separate contracts to Bell Helicopter and Sikorsky Aircraft to develop, manufacture, and test helicopters constructed primarily of advanced composite materials. Crash tests of the Bell and Sikorsky ACAP static test articles were conducted in 1987 at the IDRF to demonstrate their impact performance and to verify compliance with crash requirements [44-45, 47-48]. A photograph of the Sikorsky ACAP helicopter is shown in Figure 12(a).

The Sikorsky-developed KRASH model of their ACAP helicopter is shown in Figure 12(b). The model was developed to aid in the early design process [44]. It consisted of 53 discrete masses, 23 spring elements, 75 beam elements, and 44 nodes. The spring elements were used to represent the tires and landing gear stages. The impact test was performed at 39-ft/s vertical velocity, with an impact attitude of 10° pitch and 10° roll.

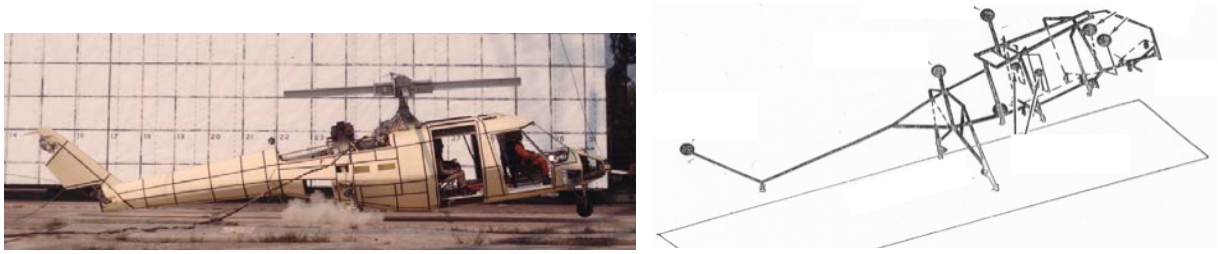

(a) Photograph of the 1987 drop test. (b) KRASH model.

Figure 12. Sikorsky ACAP crash test article and KRASH. Figures reprinted from Reference 44.

The correlation between drop test data and the pre-test KRASH simulation is presented in three categories in Reference 44. First, a comparison is provided that shows the timing of key events, such as initial right landing gear contact, left gear contact, nose gear contact, initiation of honeycomb stroking in the gears, and fuselage contact. The correlation of the timing of these events is very good. Next, comparisons of force and displacement responses of the landing gear are shown, which are also very good. Finally, the acceleration responses of the rotor transmission mass, engines, and occupants are presented. The test-analysis comparison of the vertical acceleration response of the rotor transmission mass is shown in Figure 13. The plot shows that the KRASH simulation accurately predicts the time duration and the onset rate of the acceleration pulse. However, the peak acceleration of the KRASH simulation is 25-g compared to 34-g for the experimental data. This level of agreement is considered generally acceptable today, especially for pre-test predictions.

This example is just one of many that could be illustrated in which KRASH predictions showed good correlation with test data. Part of the explanation for the high level of agreement is the fact that experimental data are used in defining the properties of spring elements that make up the model. In the case of the Sikorsky ACAP, the landing gear properties had been determined from a prior drop test of the landing gear alone [46]. Also, the model was developed such that the inertial properties of the test article, i.e. total weight and center-of-gravity location, were matched exactly. Given these factors, one would expect that the response of the high mass items such as the engines and rotor transmission would be well predicted. Once a model, such as the Sikorsky ACAP helicopter model,

is validated, it can be used to predict the response of the airframe to a variety of other impact conditions within a limited range of parameters.

Illustrative Example of Test and Analysis Comparison: LS-DYNA

In March 2010, a full-scale crash test of a MD-500 helicopter was performed at NASA Langley's LandIR facility. The purpose of the test was twofold: to evaluate the performance of an external Deployable Energy Absorber (DEA) [50-60] and to assess the ability of LS-DYNA to predict the impact responses of the DEA, the airframe, and the seated ATDs, based on an integrated finite element model. This simulation was one of the first system integrated models developed and executed at NASA. Measured impact conditions were 25.6-ft/s vertical and 38.8-ft/s horizontal with -5.7° pitch, 7.0° roll, and 9.3° yaw attitude at impact. Although this impact condition is severe, it is still considered survivable. Additional details regarding the test and simulation may be found in Reference 60. A photograph of the test article is shown in Figure 14.

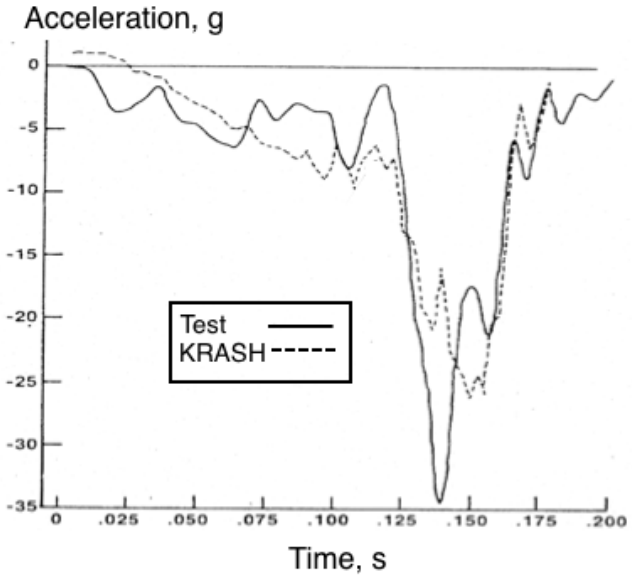

Figure 13. Comparison of the vertical acceleration responses of the rotor transmission mass.

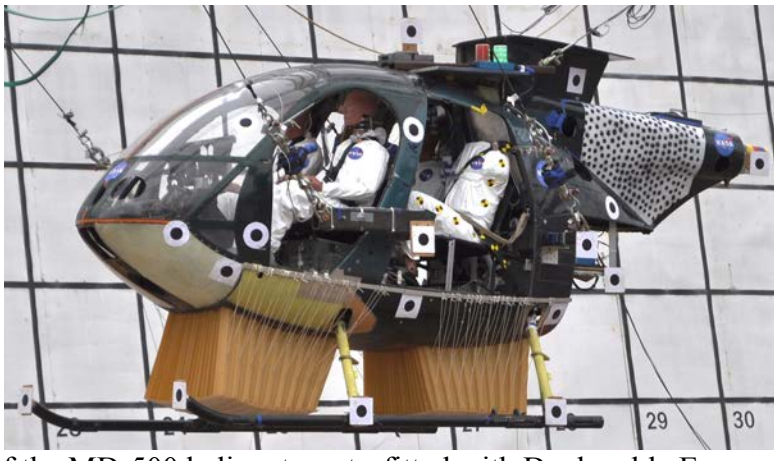

Figure 14. Photo of the MD-500 helicopter retrofitted with Deployable Energy Absorbers (DEA).

The MD-500 helicopter is designed to seat four occupants, two crew and two passengers. The total weight of the test article, including the DEA, was 2,940 lb. Four instrumented ATDs were used to represent the two crew and two passengers. The pilot in the front left crew position was a 50th percentile Hybrid III male ATD. The copilot in the front right crew position was a 50th percentile Hybrid II male ATD, and the rear passenger on the left side was a 50th percentile Hybrid II male ATD. The Hybrid II and III ATDs weighed 170-lb each. For the right rear passenger, a specialized Human Surrogate Torso Model (HSTM) developed by the Johns Hopkins University-Applied Physics Laboratory (JHU-APL) was used. The biofidelic HSTM contained detailed representations of thoracic organs, skeletal structure, and soft tissue which is mated to the pelvis and legs of a 50th percentile Hybrid III male ATD. The HSTM/Hybrid III ATD weighed 170 lb.

The fuselage and skid gear were instrumented with a combination of strain gages and accelerometers. ATD instrumentation included head, chest, and pelvic accelerometers, lumbar load cells, restraint load cells, and pressure gages. Data, totaling 160 channels, were collected at a sampling rate of 10,000 Hz. Measurements of vehicle kinematics were recorded using 2- and 3-dimensional large field photogrammetry. A detailed description of the test results is provided in Reference 54.

A critical component evaluated in the impact test was the externally mounted DEA, which was conceived and patented by Dr. Sotiris Kellas of NASA Langley [50]. The DEA is constructed of Kevlar-129 fabric and consists of multiple hexagonal cells. Two DEA blocks, spanning the fuselage belly surface, were secured to the fuselage outer skin with parachute cord. The flexible honeycomb design allows the DEA to be stowed flat external to the fuselage belly and to be deployed into the hexagonal configuration during an emergency. In this way, the DEA concept is similar to external airbags, providing extra energy absorption to the airframe when needed. In the deployed configuration, the DEA is loaded along the normal axes of the cells causing them to permanently deform under load and absorb energy. When loaded, the cell walls fold to form a controlled accordion-like pattern.

A computer aided design geometry model of the MD-500 fuselage was provided by the US Army AATD, as a starting point for model development. The geometry model consisted of surface representations of the fuselage outer mold line. Additional details of the interior structure, such as the fuselage frames and the keel beam, were developed based on hand measurements. To keep the computational time low, the element count for the integrated model was targeted not to exceed 500,000 elements, including seats and occupants. The fuselage model was composed of shell elements representing airframe skins, ribs and stiffeners. Ballast weights representing rotor mass, tail mass, and fuel were incorporated into the model as concentrated mass elements.

Two crew seats and a single passenger bench seat were installed in the airframe. The seats are standard military issue with aluminum frames and nylon mesh fabric stretched over the frames. The seat geometry was reconstructed using 3-dimensional photogrammetric techniques. The models of the crew and passenger seats are illustrated in Figure 15. Finite element models of the 50th percentile

Hybrid III male were used to represent the Hybrid II and III ATDs [61]. These models contained a combination of rigid and deformable elements for body parts. Using the LS–DYNA preprocessor, the ATD models are easily imported and positioned within the helicopter model. The LSTC occupant model contained 4,295 elements and is shown in Figure 16(a).

Figure 15. Depiction of crew and passenger seat models.

A reduced human torso model was constructed and adapted from JHU-APL's detailed Human Torso Finite Element Model (HTFEM) [62]. This model includes organs and soft tissue components made from solid silicone elements; and the sternum, ribcage, vertebrae, and scapula are modeled with fiberglass beam and shell elements. The reduced HTFEM, depicted in Figure 16(b), was attached to the LSTC Hybrid III pelvis and legs, and the total model contained 8,034 elements. The pilot and copilot models are restrained with four point harnesses, and the passenger model and reduced HTFEM are restrained with three point harnesses.

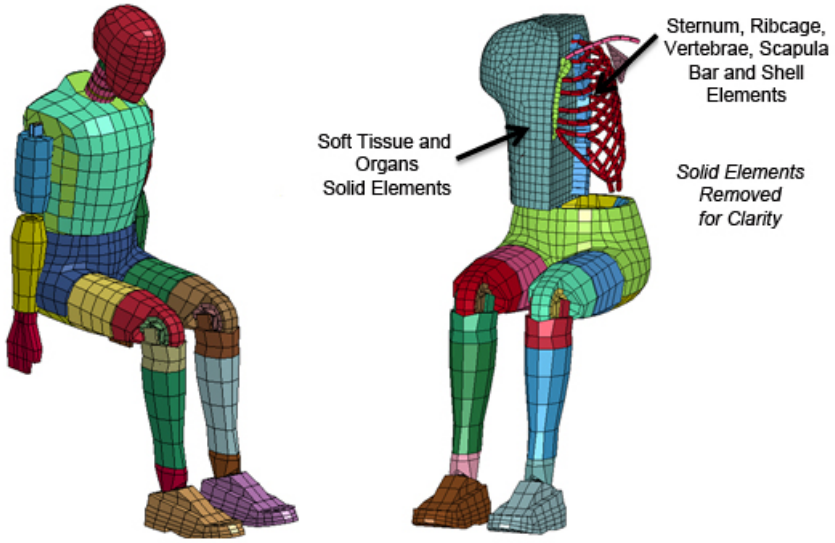

(a) LSTC Hybrid III model. (b) HTFEM/Hybrid III dummy model.

Figure 16. Dummy finite element model depictions.

The system-integrated MD-500 finite element model with the DEA is shown in Figure 17. This model had approximately 400,000 elements in total, with 266,000 elements representing the DEA. The model size is commensurate with automotive crash model sizes. For a simulation time of 0.2 seconds, the system-integrated MD-500 model runtime was approximately 24 hours, with execution on a Linux-based workstation computer with 8 processors running LS-DYNA version 971 Symmetric Multi-Processing (SMP).

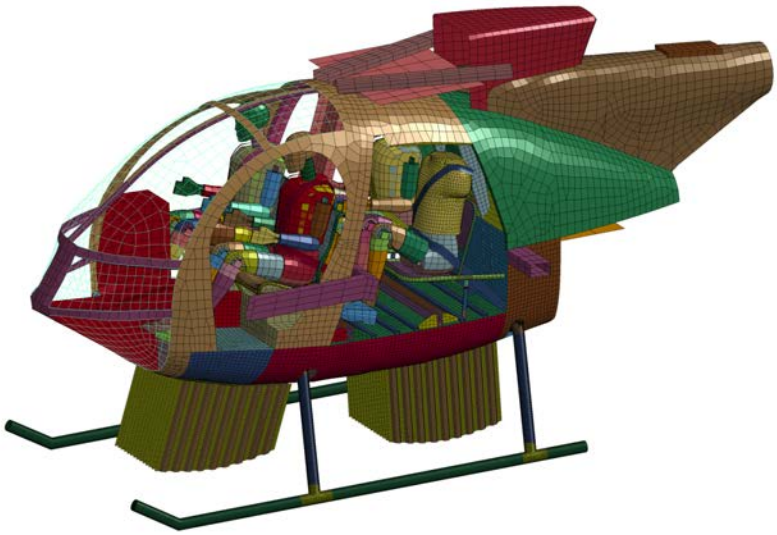

Figure 17. MD-500 system-integrated finite element model.

The impact orientation and deformation at peak acceleration are shown in Figure 18 for test and analysis. Qualitatively, the global deformation pattern of the DEA model was similar to the deformation observed from the high-speed video, which included folding on the right side and crushing on the left side, relative to the passenger's view. In the simulation, dimpling of the skin occurred in the region above the rear DEA, whereas post-test inspection of the test article revealed no damage. During the test, the DEA exhibited folding, crushing, and sliding along the belly, which was attributed to the presence of roll attitude and shear loading. This behavior was only partly captured by the shell-based DEA model.

Despite the qualitative differences between local deformation patterns, reasonable agreement is obtained between the simulation and the overall response of the test article. At time = 0.0-s, the skid gear initially impacts the surface. At time = 0.03-s, the DEA begins to attenuate energy. As expected from previous testing of the DEA, vertical accelerations of the airframe are effectively trapezoidal in shape. In this manner, the DEA performs as a load limiting shock absorber, regulating the loads between 10- and 15-g and expanding the deceleration pulse duration through crushing and folding.

Test and analysis acceleration responses are plotted in Figure 19(a), and changes in vertical velocity are plotted in Figure 19(b) at the centerline of the floor beneath the passenger seats. At this location, the model does a good job of predicting the initial peak acceleration and the pulse duration. The test response shows a second peak acceleration at approximately 0.0125-s, which occurs earlier in time

for the predicted response. The velocity change responses are similar initially. At 0.065-s, the two curves begin to deviate slightly, with the simulation model removing velocity more quickly than the test. However, by the end of the pulse the two curves are in close agreement once again.

(a) MD-500 prior to initial impact. (b) MD-500 at peak acceleration.

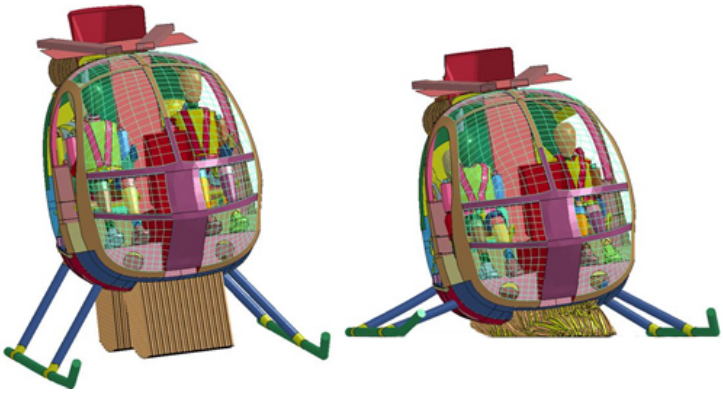

(c) Model prior to impact. (d) Model at peak acceleration.

Figure 18. Test-analysis depictions at a time just prior to impact and at peak acceleration.

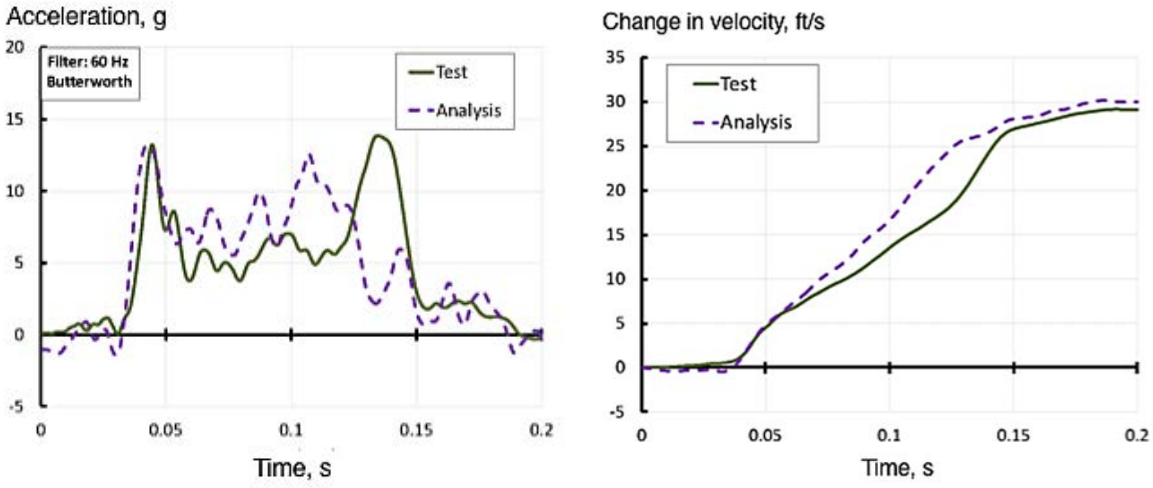

(a) Acceleration responses. (b) Velocity responses.

Figure 19. Comparison of test and analysis, centerline of the floor beneath the passenger seats.

The predicted and experimental pilot pelvic vertical acceleration responses are shown in Figure 20. The peak acceleration from the analysis is over twice the magnitude of the test response and the pulse shape is also different. These results provided the first indication that the ATD models, which were developed originally for automotive crash simulations, were not calibrated for the dominant vertical loading environments experienced in a rotorcraft crash.

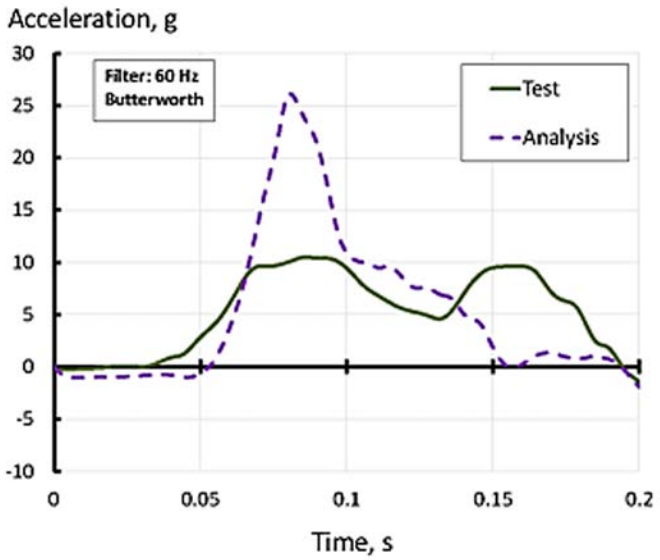

Figure 20. Comparison of test and analysis, pilot pelvis vertical acceleration.

The LS-DYNA simulation effort described in this section of the paper actually spawned some follow-on work. First, the test-analysis comparisons for the original model were somewhat unsatisfactory. Consequently, a more computationally rigorous formulation was applied to results from a second MD-500 test, conducted without the DEA, to calibrate the model. Fundamental to the success of the model calibration effort is the ability of the model to predict the observed behavior in the presence of modeling uncertainty. Although there is no universally accepted metric to judge model adequacy, the approach used following the second test incorporates uncertainty propagation and quantification to assess model adequacy. In the end, a parameter set was developed and judged based on the probability of being able to reconcile the test with the analysis. Results from this effort highlighted model deficiencies that were unexplainable without additional component data. This work is described in Reference 60. Additional information regarding this method of test-analysis quantification is described in References 63 and 64.

The second follow-on work relates to the inadequacy of LSTC-provided ATD finite element models. As noted previously, these models were calibrated for automotive crashes in which loading to the occupant is primarily normal to the spine, whereas loading in aircraft/rotorcraft crashes is primarily parallel to the spine. As a result of the poor performance of the Hybrid III dummy model, an experimental program was conducted in which a series of 14 vertical impact tests were performed using Hybrid III 50th percentile and Hybrid II 50th percentile ATDs [65]. The purpose of conducting these tests was threefold: to compare the impact responses of Hybrid II and Hybrid III ATDs under

two different loading conditions, to compare the impact responses of the Hybrid III configured with a nominal curved lumbar spine to that of a Hybrid III configured with a straight lumbar spine, and to generate data for comparison with predicted responses from two commercially available ATD finite element models. The two loading conditions examined were a high magnitude, short duration acceleration pulse, and a low magnitude, long duration acceleration pulse, each created by using different paper honeycomb blocks as pulse shape generators in the drop tower. The test results show that the Hybrid III results differ from the Hybrid II results more for the high magnitude, short duration pulse case. Comparison of the lumbar loads for each ATD configuration show drastic differences in the loads seen in the spine. The analytical results show major differences between the responses of the two finite element models. These tests were later repeated for the more advanced THOR dummy [66].

ATD Occupant Models

Any discussion of crash modeling and simulation would not be complete without touching on the significant advancements that have been made in ATD modeling. In the 1960's and 1970's a significant amount of work was performed to develop dynamic models for use in crash analyses. These models varied greatly in complexity, with up to 40 degrees of freedom, different numbers of body segments and joints, and based on either Lagrangian equations of motion or Eulerian rigid body equations. In general, these models contained contact algorithms to sense contact between the body (elliptical shapes) and seat belts and/or surrounding structure, such as cabin interiors. Joints were typically represented as hinges or ball-and-socket.

Several of these early ATD models are shown in Figure 21. Cornell Aeronautics Laboratory Three Dimensional (CAL3D) was developed at Cornell University and sponsored by the Department of Transportation and the Motor Vehicle Manufacturer's Association [67]. It contained 15 body segments with 40 degrees of freedom. In 1972, airbag modeling capability was added. The model also simulated contact and contained rudimentary injury prediction capability. The 1975 version of CAL3D was renamed Articulated Total Body (ATB) when the US Air Force assumed further development of the model. Subsequent releases of ATB added water force capability. The code was written in FORTRAN90 and was executable on many computer platforms, including PCs. UCIN-3D was developed at the University of Cincinnati and was sponsored by the Office of Naval Research [68]. This model contained 12 body segments constructed of frustrums of elliptical cones, elliptical cylinders, and spheroids. Finally, PROMETHEUS was developed by Boeing under sponsorship by the Office of Naval Research [69]. PROMETHEUS simulates a crash victim using either a 2-dimensional seven-link side-facing model, or a 3-dimensional eleven-link forward-facing model, which is shown in Figure 21(c).

In about the same time period, an ATD occupant model was being developed at Penn State University that eventually became Seat/Occupant Model-Light Aircraft (SOM-LA) [70, 71]. Further development of SOM-LA was performed at Simula Incorporated under FAA sponsorship. The model contained 11 rigid mass segments corresponding to the mass distribution shown in Figure 22(a).

Connectors between the rigid masses were represented as hinges or ball-and-socket joints. The model contained 31 degrees of freedom. Contact surfaces in the model are depicted in Figure 22(b). The initial model was released in 1975; however, modifications have been made to improve simulation quality, increase capability and to add additional output [72, 73]. In the 1980's, SOM-LA was modified to created Seat/Occupant Model-Transport Aircraft (SOM-TA) [74].

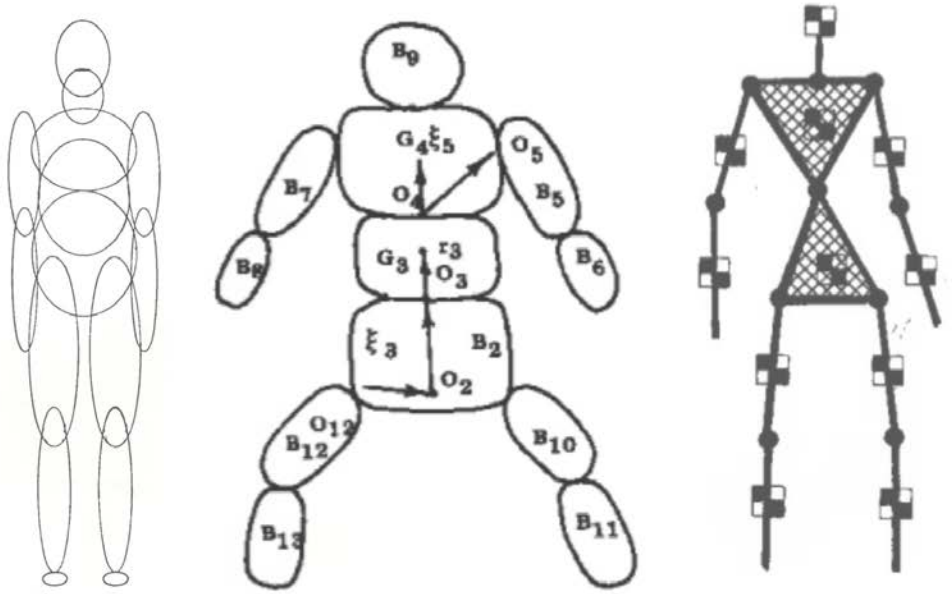

(a) CAL3D (b) UCIN-3D (c) PROMETHEUS

Figure 21. ATD models developed in the 1960's and 1970's. Reprinted from References 66-68.

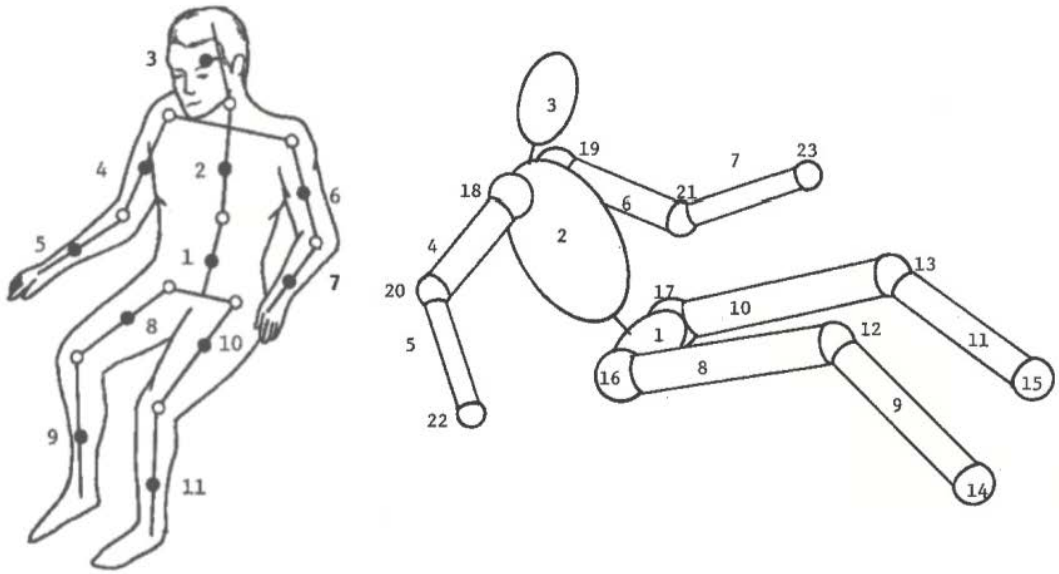

(a) Human mass distribution (b) Contact surfaces in SOM-TA

Figure 22. Early depictions of the SOM-LA model. Reprinted from Reference 70.

In the mid-1970's, the Research Institute for Road Vehicles TNO, in conjunction with the Netherlands Institute for Road Safety Research, entered a six-year program to develop an occupant model designated MAterial DYnamic MOdel (MADYMO). MADYMO used the Lagrangian formulation to solve the equations of motion and had added flexibility in the selection of the number of body segments and joints needed for the simulation [75, 76]. Yet, it remained a gross-motion 3-dimensional occupant model.

All of the models mentioned above are essentially derived on the basis of rigid body dynamics. Today, given the development of fast computer hardware and software, finite element codes now incorporate occupant models that are constructed of finite elements, making it possible to simulate occupant deformations during impact. In the finite element model, deformable parts are modeled as flexible bodies and are covered with faceted surfaces to better resemble the ATD dummy body. These later models contain a wide variety of joints including revolute, translational, spherical, universal, cylindrical, planar, bracket, and free. In general, the models are available for execution within the commercial codes, LS-DYNA, NASTRAN SOL 700, and PAM-CRASH.

Two of the ATD models that are available in LS-DYNA today are shown in Figure 23. These models contain varying degrees of complexity. For example, the Hybrid III Fast model, shown in Figure 23(a), is created with fewer elements (about 4,000) to allow for quicker execution time, whereas the detailed model, shown in Figure 23(b) has many additional elements (450,000+) to represent the ATD. The detailed model is available for a 5th percentile female and a standing 50th percentile male.

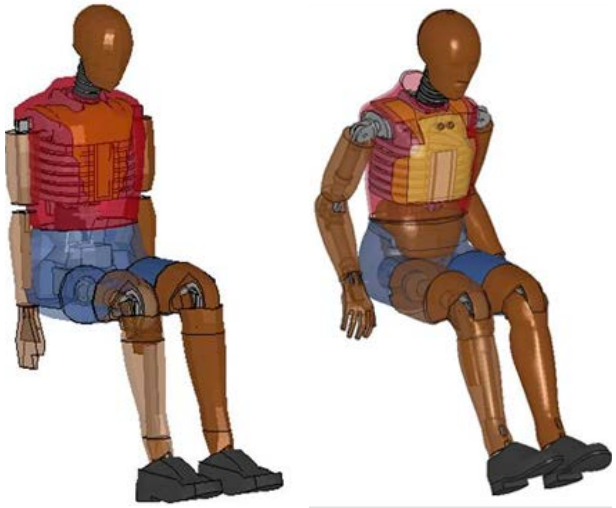

(a) Hybrid III Fast. (b) Hybrid III Detailed.

Figure 23. LS-DYNA ATD models currently available.

The current trend today is to not only model the ATD, but to model the human body and to be able to predict brain concussion, aortic rupture, and other types of soft tissue injury. Some of these models are based on MADYMO and ATB, and some are developed as separate codes, such as the human body model developed by Global Human Body Model Consortium (GHBMC) [77, 78], and the Total Human Model for Safety (THUMS) [79]. Founded in 2006, GHBMC is an international consortium

of automakers and suppliers working with research institutes and government agencies to advance human body modeling technologies for crash simulations. THUMS is a finite element model of the human body intended for injury analysis. The model was jointly developed by Toyota Motor Corporation and Toyota Central Research and Development Laboratories, Incorporated. Depictions of the GHBMC and the THUMS are shown in Figure 24. Unfortunately, these models contain on the order of 1,000,000 nodes and 1,750,000 elements, making it impractical to incorporate them into existing vehicle models for crash simulations. At this time, it is easier to use the current Fast ATD model, shown in Figure 23(a), to generate occupant loading, which can be applied subsequently as input conditions in stand-alone simulations using the human body models.

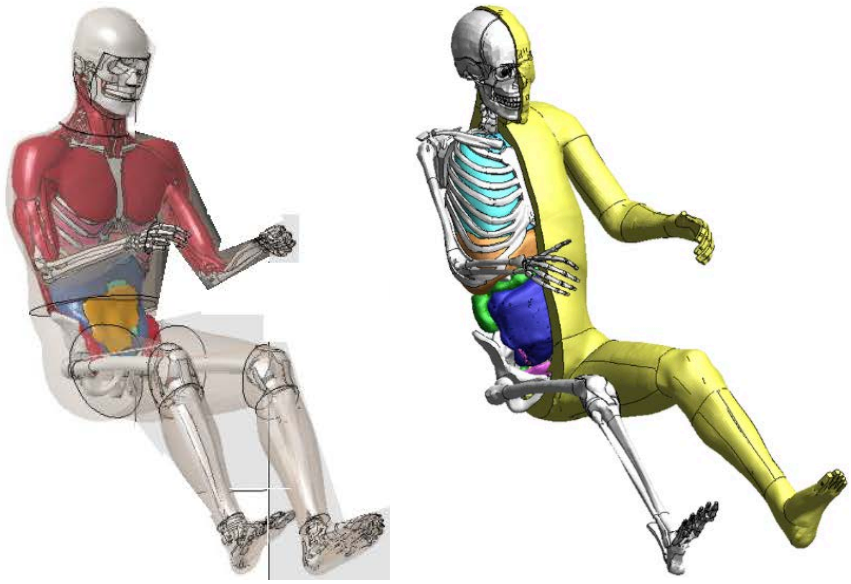

(a) GHBMC model. (b) THUMS model.

Figure 24. Human body models for crash impact analysis.

Multi-Terrain Simulation

Since fewer than 20% of helicopter accidents occur onto a smooth prepared surface [4, 80], it is imperative that analytical codes include capabilities for modeling other terrain besides rigid surfaces. LS-DYNA is capable of simulating water impacts using a variety of methods. These include ALE, SPH, and EFG. Often bird strike simulations are performed in which the "soft" bird is modeled using SPH [81]. In 2008, NASA conducted a vertical drop test of a prototype composite fuselage section, outfitted with DEA, into water and LS-DYNA simulations were performed using both ALE and SPH [82]. The fuselage section and two models are depicted in Figure 25. The ALE model matched the acceleration onset rate; however, the peak value was slightly over predicted. The level of correlation improved when a 1°-roll attitude was incorporated into the model. These results demonstrate the importance of accounting for experimental eccentricities in the model to achieve optimal correlation. The SPH model was used to simulate three different (3-, 2-, and 1.5-in.) mesh densities for the water. The results for the drop test of the fuselage section with DEA indicated that the 2-in. mesh spacing

provided the best correlation with test data. This finding was unexpected in that the finest SPH mesh did not yield the most accurate results. See Reference 82 for additional information.

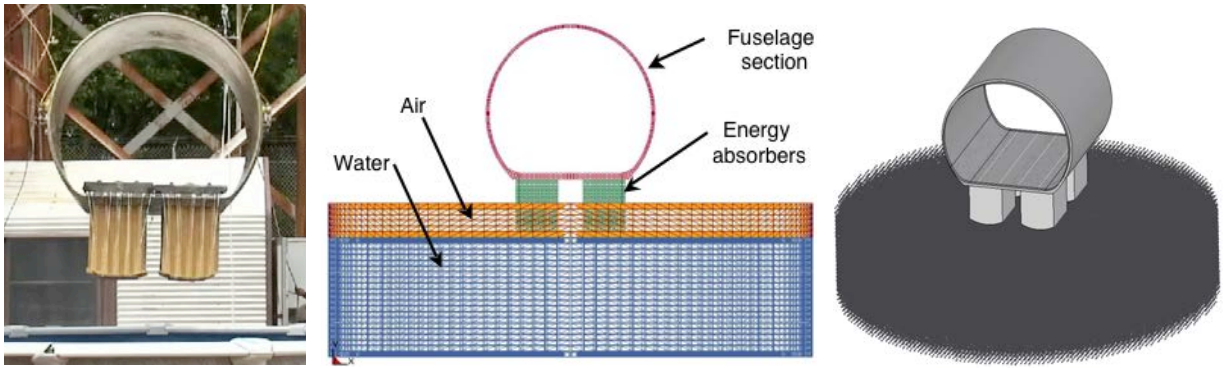

(a) Drop test photo. (b) ALE model. (c) SPH model (2-in. spacing).

Figure 25. 2008 vertical drop test and models of a composite fuselage section into water.

In 2013 and 2014, full-scale crash tests of CH-46E helicopters were performed at NASA's LandIR facility onto soft soil as part of the TRACT program. The LS-DYNA model of the TRACT 2 test article is shown in Figure 26. The soil was represented using solid elements that were assigned Material Model 5 (*MAT_SOIL_AND_FOAM) in LS-DYNA®, which is a material model for representing soil and foam [83]. The soil block was 24-in. deep by 148-in. wide by 600-in. long. A coefficient of friction of 0.5 between the airframe and the soil was used in an automatic single surface contact definition. Initially, the soil was represented as a single block with one material model assigned; however, based on soil characterization test results, the model was changed to a layered soil configuration. The top 3-in.-deep layer of soil was represented using Mat 5 with input properties obtained from soil tests conducted on gantry unwashed soil, which were performed for the Orion program [84]. The bottom 21-in. deep layer was also represented using Mat 5 with input properties of sand, whose bearing strength matched in-situ test results conducted prior to and after the TRACT 2 crash test. The bottom and side nodes of the soil model were fully constrained from motion in LS-DYNA [85].

Figure 26. LS-DYNA model of the TRACT 2 impact test.

The recent TRACT test was conducted on a bed of soil over concrete that provided both realistic forward and vertical crash accelerations. Unfortunately, modeling soils is a very difficult task as the material properties are highly variable with moisture content, soil packing treatments, particle size, and clay/sand mixture, which can be non-homogeneous from one location to another. The soil density was measured pre-test and instrumented hemispheres were dropped to assist in soil characterization. The soil was a mixture of sand and clay and had been characterized by a soil laboratory; however, the data generated were only a snapshot of the reconstructed soil at a given moisture level. Unloading of the soil is particularly hard to replicate as it influences the rebound of the structure. Material model 5 uses a simple unloading curve with constant stiffness. Figure 27(a) illustrates a model used to simulate a hemisphere impacting onto soil. A high value for the unloading slope was used for this simulation. Comparison of the test and analysis acceleration responses are shown in Figure 27(b). Although the peak accelerations are close in magnitude, the predicted pulse shape is not representative of the measured shape. The predicted acceleration matches the test response during the early part of the pulse; however, the peak acceleration is maintained too long in the model and the unloading is not properly matched. These results indicated that the parameters used in the model for the soil do not accurately replicate the actual material properties. This example highlights the fact that modeling of soil impacts is challenging, even with soil characterization test data available.

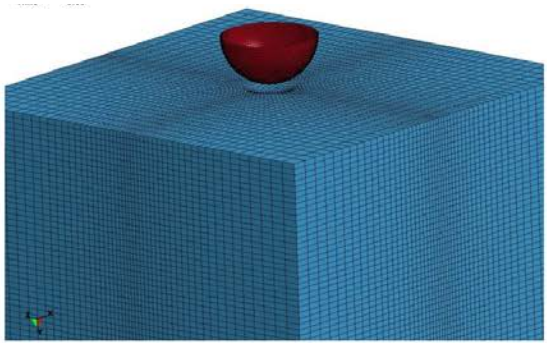

(a) Penetrometer model impacting soil.

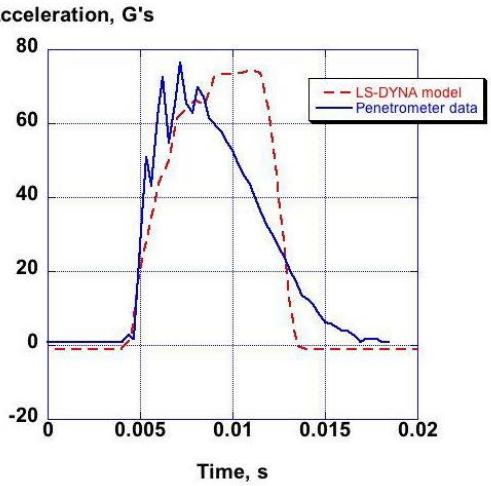

(b) Test-analysis comparison.

Figure 27. Soil material characterization model with test-analysis comparison.

LS-DYNA Today

Currently, LS-DYNA is used to perform a myriad of simulations. Some of the capabilities of LS-DYNA include: Full 2-dimensional and 3-dimensional finite elements; nonlinear and rigid body dynamics; quasi-static simulations, vibration modes, linear static analysis, and thermal analysis; fluid-structural interaction capabilities including Eulerian fluids, ALE, Navier-Stokes fluids, compressible fluid solver, SPH, and EFG; underwater shock, failure analysis, and crack propagation; and, real-time acoustics, implicit spring back, multi-physics coupling, structural-thermal coupling, adaptive remeshing, radiation transport, and electromagnetism. The capabilities of the LS-DYNA code

continue to be expanded, including improvements in pre- and post-processing software for model building and assessment. Today, LS-DYNA is more than an explicit, transient dynamic finite element code for crash simulation, it has become a true multi-physics analysis code.

ROTORCRAFT STRUCTURAL DESIGN FOR CRASHWORTHINESS

During the past 4 decades, several research and development programs have been sponsored by the US Army AATD to encourage the use of advanced composite materials in rotorcraft structural design. The first program was the ACAP [43-49]. The purpose of this program was to demonstrate the potential of advanced composite materials to save weight and cost in airframe structures while achieving systems compatibility and meeting military requirements for vulnerability reduction, reliability, maintainability, and survivability. The ACAP began in 1979 and concluded in 1987 with the crash tests of the Bell and Sikorsky static test articles at the IDRF. Both the Bell and Sikorsky ACAP helicopters are described in this section of the paper as excellent examples of the systems approach to crashworthy design.

In 2008, a second developmental program, designated the Survivable Affordable Repairable Airframe Program (SARAP) Virtual Prototype and Validation (VPV) Program, was initiated between Sikorsky Aircraft and the US Army AATD. The objectives of the program were to validate technology advances in design processes, structural efficiency, crashworthiness, materials and manufacturing processes, and reparability of rotorcraft airframe structures. Specific objectives of the SARAP VPV program included a 25% weight reduction, 40% recurring and 40% non-recurring cost reduction, maintaining crashworthiness, and repairable structure as compared to a 2002 metallic baseline. The comprehensive SARAP VPV program, which is described in Reference 86, included identification, review and evaluation of various design, analysis, material, and manufacturing technologies. As part of this program, a prototype Technology Validation Article (TVA) was constructed of composite materials and was designed to replicate the center section of a metallic UH-60 Black Hawk helicopter. In this section of the paper, each of the development programs (ACAP and SARAP) will be reviewed, especially focusing on the application of composite materials in crashworthy helicopter design.

ACAP

Crash tests of the Bell and Sikorsky ACAP static test articles were conducted in 1987 at the IDRF to demonstrate their impact performance and to verify compliance with crash requirements. A pre-test photograph showing the two ACAP helicopters at the IDRF is shown in Figure 28. The Sikorsky version is shown on the right side of the figure, while the Bell version is shown on the left side. Photographs taken during the impact tests are shown in Figure 29. These tests demonstrated the successful application of composite materials to save weight and maintenance costs in rotorcraft design, while achieving improved crash protection.

The Bell ACAP helicopter, designated the Model D292, had a gross weight of 7,525-lbs. The onboard dynamic systems including the engines, rotors, transmission and flight controls were taken from the

Bell Model 222 commercial helicopter. The Sikorsky S-75 ACAP helicopter had a gross weight of 8,470-lbs and utilized the dynamic systems and subsystems of the Sikorsky S-76 commercial helicopter.

Figure 28. Photograph of two ACAP helicopters, Bell version (left) and Sikorsky version (right).

(a) Photo of the Bell ACAP during crash test.

(b) Photo of the Sikorsky ACAP during crash test.

Figure 29. Photographs of the Bell and Sikorsky ACAP helicopters taken during crash testing.

As described in References 47 and 48, the Bell ACAP helicopter was fabricated as a semimonocoque structure with damage tolerant and crash resistant features. The composite materials used in its construction included Kevlar/epoxy, fiberglass/epoxy, graphite/epoxy, Kevlar-graphite/epoxy hybrid, Nextel/polyimide, and graphite and/or fiberglass/bismaleimide. Composite materials were selected for each component to be best suited for the particular application and anticipated loading environment.

In the Bell ACAP, the primary energy absorbing components were the main landing gear and the tail gear. The main landing gear were designed with two stages. The first stage consisted of oleo shock struts, which provided energy absorption to attenuate loads and prevent the fuselage from contacting the ground for a 20-ft/s velocity impact. The second stage consisted of crushable graphite/epoxy tubes

on the main gear and a tube cutter on the tail gear to provide additional energy absorption for crash impacts up to 42-ft/s. The fuselage structure was designed to provide a protective shell surrounding the occupants that consisted of three stiff and strong bulkheads, surrounded underneath by crushable structure. The Bell ACAP utilized composite sandwich energy absorbers fabricated of Kevlar/epoxy face sheets and Nomex honeycomb core, as shown in Figure 30. Initiators were used to enable the sandwich structure to crush without generating high initial loads. The addition of load-limiting seats and restraint systems completed the crashworthy design of the Bell ACAP.

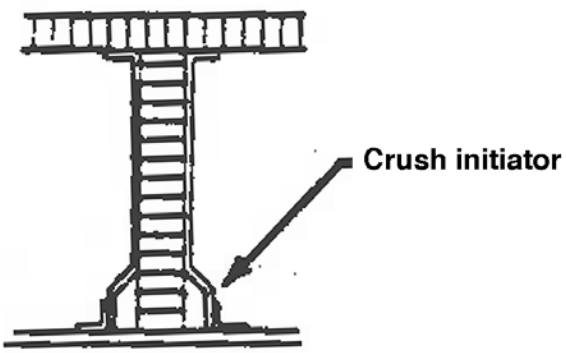

Figure 30. Schematic of the composite sandwich energy absorber used in the Bell ACAP. Reprinted from Reference 47.

A full-scale crash test of the Bell ACAP helicopter static test article was conducted on August 27, 1987. Unfortunately, this test was an aberration in that no data were collected due to premature release of the umbilical cable. However, photographic data were recorded from high-speed cameras. The measured impact conditions were: 41.4-ft/s vertical velocity, 26.4-ft/s forward velocity with 15° pitch (nose up) and 14.5° roll (right side down) [47, 48].

Despite the fact that no data were collected, several important findings were made based on examination of the post-test article. The first finding was that the rotor transmission mass was retained and did not intrude into the occupied cabin. The protective shell surrounding the occupants was maintained. The energy absorbers located on the right side of the helicopter were fully crushed, which is expected since the right side of the helicopter impacted first due to its roll attitude. There was less crushing observed on the left side. The crew and troop seats stroked within the 12-in. available stroke and did not bottom out. The right and left main gear exhibited crushing of the graphite tubes, but also did not bottom out. Finally, the fuel tanks did not leak during or after the test. Thus, the full-scale crash test of the Bell ACAP was a successful demonstration of a crashworthy composite helicopter.

The primary crashworthy features of the Sikorsky ACAP helicopter were the main and nose landing gear. The landing gear were a tricycle arrangement designed for a 12.5-ft/s vertical velocity for normal landing and 42-ft/s vertical velocity for a crash landing. Crash protection is provided by a two-stage shock strut in which the first stage is a conventional air-oleo design and the second stage consists of a crushable 25-in.-long honeycomb canister. An upper set of pins in the landing gear

protects the honeycomb from being crushed until the oleo stage has stroked 12 in. Finally, the attachment fittings that connect the landing gear to the fuselage were designed to exhibit bearing failures to absorb additional energy after the gear is fully stroked. Another crashworthy feature of the helicopter is the crushable lower portion of the keel beams and transverse bulkheads. Two inner and two outer keel beams were located beneath the floor and were constructed of two horizontal C-channels, one above the other with a beaded or waffle web geometry, as shown in Figure 31. The upper channel was constructed of graphite and was designed to support the floor. The lower 4-in.-high portions of the keel and bulkhead beams were made of a thinner beaded Kevlar, which was designed to crush and absorb energy.

A vertical drop test of the Sikorsky ACAP static test article was performed at the IDRF on September 17, 1987, as depicted in Figure 29(b). The test article was dropped from a height of 23.6-ft providing an impact velocity of 39-ft/s with an impact attitude of 10° nose-up pitch and a 10° right down roll. As reported in Reference 45, the magnitudes of floor-level, seat, and occupant accelerations were found to be in the survivable range. Also, main landing gear failure of the forward side brace occurred and permitted the gear to rotate and produce premature bearing failure of the landing gear attachment. As a result, the amount of energy absorption contributed by the main landing gear was reduced, but was compensated for by crushing of the subfloor.

Figure 31. Photograph of the Sikorsky ACAP helicopter energy absorbing subfloor design.

As a final note, the Sikorsky ACAP flying prototype helicopter was crash tested at the IDRF in 1999. The test was conducted at 38-ft/s vertical velocity and 32.5-ft/s forward velocity onto concrete for a resultant velocity of 50-ft/s. The primary objective of the test was to provide experimental data for validation of an explicit, transient dynamic finite element simulation. All crashworthy features in the airframe performed well during the test [87].

SARAP VPV

A TVA was constructed by Sikorsky Aircraft as part of the SARAP VPV program, which addressed multiple design, risk assessment, and manufacturing goals [86]. The TVA was manufactured primarily of graphite unidirectional tape composite with a thermoplastic resin system; however,

portions of the framed fuselage section were constructed of a plain weave graphite fabric material with a thermoset resin system. The TVA was approximately 6-ft tall and 7.5-ft long. Instead of incorporating crushable subfloor structure, as was done with the Sikorsky ACAP helicopter, a novel "Tilting Roof" concept was developed and incorporated into the TVA. As stated in Reference 86, "the basic principle of the Tilting Roof was to engineer into the cabin design an area where energy attenuating features, such as crushable tubes, could be located to allow the roof structure and high mass items to fail in a predictable and controlled manor. The basic system operation allows the roof structure to rotate about the forward frame area, with failures along the aft side frames allowing the tubes on the aft bulkhead to crumple and dissipate the energy associated with the crash event. The joints at the forward hinges and the side frames are designed to react flight and landing loads, but the increased forces associated with a crash are sufficient to initiate failures that lead to energy absorption."

Both static and dynamic impact tests of the full-scale TVA were performed to validate the design. The TVA was installed in the structural test stand at the US Army AATD. Following installation, forces were applied to the TVA to represent a spectrum of flight loads using actuators located at the transmission attachment points. The results from these load cases were compared to finite element simulations, which confirmed that the analytical predictions matched the test data within 10% [86].

Next, a full-scale vertical impact test of the TVA was performed at the LandIR facility in August 2008. Pre- and post-test photographs of the TVA are shown in Figure 32. The purpose of the test was to evaluate the performance of the "tilting roof" concept, patented by Sikorsky Aircraft, that was intended to dissipate the kinetic energy of high mass items, such as the rotor transmission, during a crash event [86]. Energy absorption for the tilting roof concept was provided by aluminum crush tubes, which typically display stable crushing under compressive loading. The test article weighed 5,034 lbs. and was dropped vertically onto concrete at 21-ft/s velocity.

(a) Pre-test photograph. (b) Post-test photograph showing roof collapse.

Figure 32. Pre- and post-test photos of the SARAP TVA.

Post-test inspection of the TVA indicated that damage was primarily limited to the roof area, with little or no damage found in the subfloor, or the forward framed fuselage section. The tilting roof concept failed to work as planned due to premature failure of attachment fittings. In 2010, NASA Langley obtained the residual SARAP hardware for testing under the NASA Subsonic Rotary Wing crashworthiness research program. In May 2011, NASA and Sikorsky signed a Space Act Agreement permitting cooperation between the two organizations to pursue common research interests including: composite material and airframe structural testing under dynamic loading; development of accurate and robust material models to predict aircraft structural response using LS-DYNA; and, validation of analytical models through test-analysis correlation. The results of this collaborative effort are documented in References 88-90.

Additional design programs are ongoing at this time such as the Combat Tempered Platform Demonstration, which is another program performed by Sikorsky Aircraft and sponsored by the US Army AATD. This program, which was initiated in 2012, focuses on the implementation of technologies to enhance the total survivability and operational durability of the UH-60M Black Hawk helicopter. Key technologies include a zero-vibration system, adaptive flight control laws, advanced fire management, durable main rotor, full-spectrum crashworthiness, and a damage tolerant airframe. In addition, the US Navy and US Marine Corps have sponsored development of the large, heavy-lift CH-53K King Stallion helicopter, which is fabricated primarily of composite materials. Crashworthy features of this helicopter include stroking landing gear and load-limiting seats.

Composite Energy Absorbers

There are several methods used to improve the crash safety of legacy rotorcraft. One approach is to add external energy absorbers such as the DEA or air bags. These approaches are successful in mitigating crash loads, but they also add weight to the airframe. Another approach is to retrofit the existing subfloor structure with crushable composite energy absorbers. In 2014, NASA conducted a second full-scale crash test of a CH-46E Sea Knight helicopter, designated TRACT 2, that was retrofitted with three composite energy absorbers located in the mid-cabin region: a corrugated web design [91, 92] fabricated of graphite fabric; a conical-shaped design, designated the "conusoid," fabricated of four layers of hybrid carbon-Kevlar® fabric [93]; and, a sinusoidal-shaped foam sandwich design, designated the "sinusoid," fabricated of the same hybrid fabric face sheets with a foam core [94]. The design goal for the energy absorbers was to achieve average floor-level accelerations of between 25- and 40-g to match the values obtained during the full-scale crash test of the CH-46E helicopter airframe, designated TRACT 1.

The corrugated web energy absorber was developed jointly by the Cooperative Research Centre for Advanced Composite Structures (CRC-ACS) and by the German Aerospace Center (DLR). As shown in Figure 33, the concept was developed using a building block approach, accompanied by modeling and simulation using PAM-CRASH. Initial crush testing was performed on trapezoidal elements. Eventually, the concept was incorporated into a fuselage section and a vertical drop test

was performed. In March 2014, NASA and the DLR entered into a cooperative research agreement to permit the corrugated web to be retrofitted into TRACT 2.

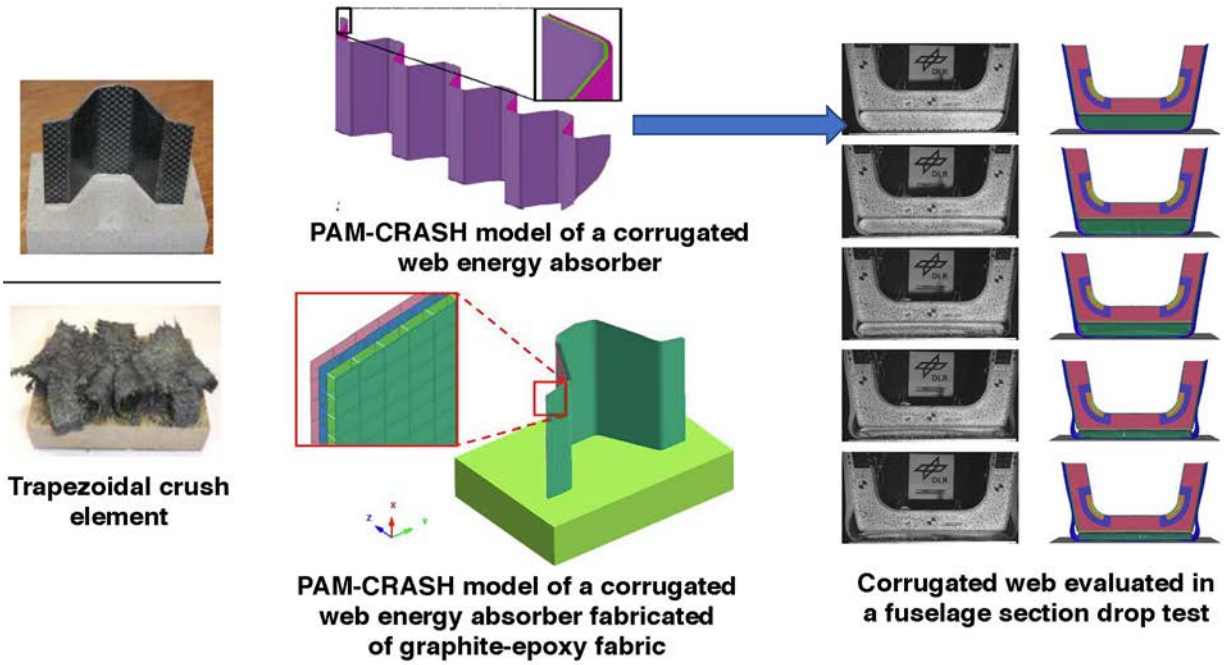

Figure 33. Development of the corrugated web energy absorber. Pictures taken from Reference 89.

NASA developed two composite energy absorbers for retrofit into TRACT 2. The first NASA-developed energy absorber is a novel conical sinusoid, or "conusoidal" composite energy absorber, also designated "conusoid." The geometry of the conusoid is based on alternating right-side-up and up-side down half-cones placed in a repeating pattern. The conusoid combines a simple cone design with sinusoidal beam geometry to create a structure that utilizes the advantages of both configurations. An isometric view of the conusoid is shown in Figure 34(a). Variations in geometry, materials, and laminate stacking sequences were evaluated during development of the conusoid and the final design consisted of four layers of a hybrid carbon-Kevlar® plain weave fabric oriented at [+45°/-45°/-45°/+45°] with respect to the vertical, or crush, direction. A photograph of a typical conusoid component is shown in Figure 34(b). Dimensions of the component are 12-in. long, 7.5-in. high, with an overall width of 1.5-in. Additional information on the development and fabrication of the conusoid energy absorber may be found in References 93 and 95.

The second energy absorber, designated the "sinusoid," consisted of hybrid carbon-Kevlar® plain weave fabric face sheets, two layers for each face sheet oriented at ±45° with respect to the vertical, or crush, direction and a closed-cell ELFOAM® P200 polyisocyanurate (2.0-lb/ft^3) foam core. Often, the actual shape of a sinusoidal energy absorber is not truly a sine wave, but a series of alternating half circles. In fact, the sinusoid concept described in this paper is actually a series of half circles with a diameter of 1.75-in.; however, the designation of "sinusoid" will continue to be used. The overall thickness of a sinusoid component was 1.5-in. with a length of 12-in. and a height of 7.5-in.

Design parameters were assessed through component testing including different materials for the face sheets and different laminate stacking sequences. Variations in sinusoid geometry were not evaluated since an existing mold was used in construction. A photograph of a sinusoid foam sandwich specimen is shown in Figure 35. Note that, in preparation for the component drop test, 0.5-in.-thick polycarbonate plates were attached to both the top and bottom surfaces of the specimen. Additional information on the sinusoid concept may be found in References 94 and 95.

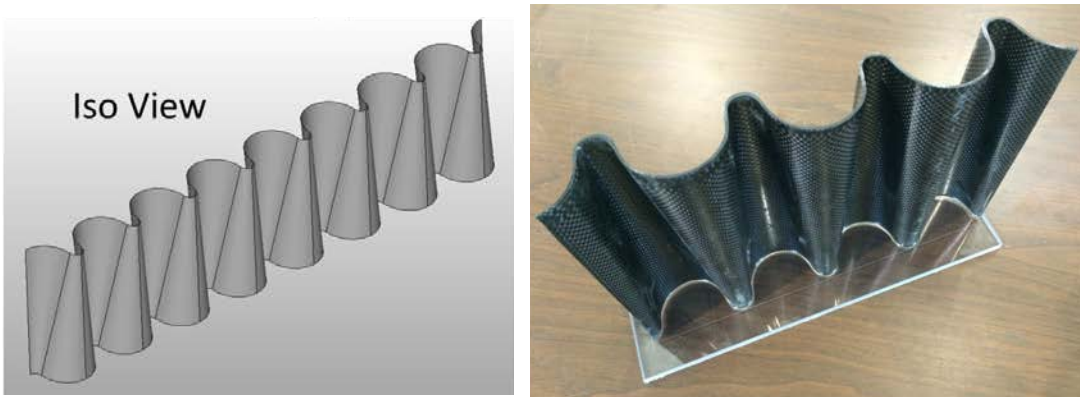

(a) Schematic drawing. (b) Photograph of component.

Figure 34. Isometric view and photograph of a conusoid component.

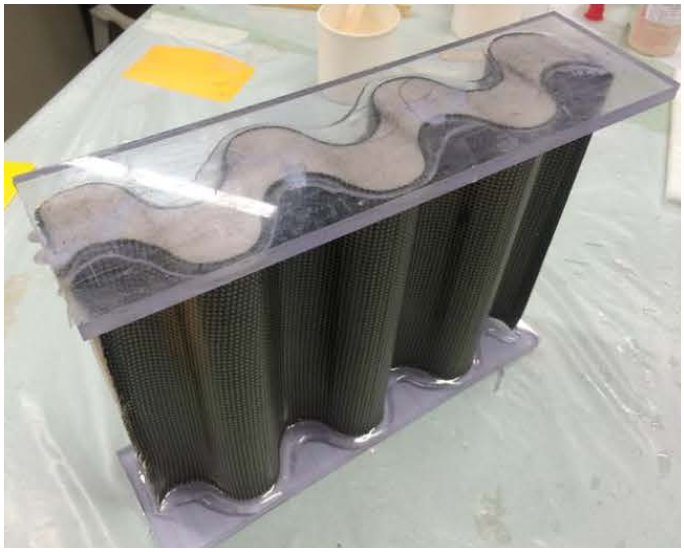

Figure 35. Pre-test photograph of a sinusoid foam sandwich component.

Both the conusoid and sinusoid energy absorbing components were subjected to dynamic crush tests using a 14-ft. drop tower. A drop mass weighing approximately 110-lb was released to impact the components at 264-in/s vertical velocity. Post-test photographs of the energy absorbers are shown in Figure 36. The identified failure mechanism for the conusoid energy absorber is folding of the walls, which is a desirable failure mode that produces a stable and constant crush response within the design level of 25- to 40-g. As shown in Figure 36(b), the sinusoid specimen exhibits stable, plastic-like deformation with uniform folding of the face sheets and crushing of the foam core. Crushing initiates along the top edge of the specimen. Note that the sides of the specimen were not covered with face

sheets, which allowed splaying of the foam core. LS-DYNA finite element models were developed of the conusoid and sinusoid energy absorbers and test-analysis comparisons were made. The simulation results are documented in Reference 95.

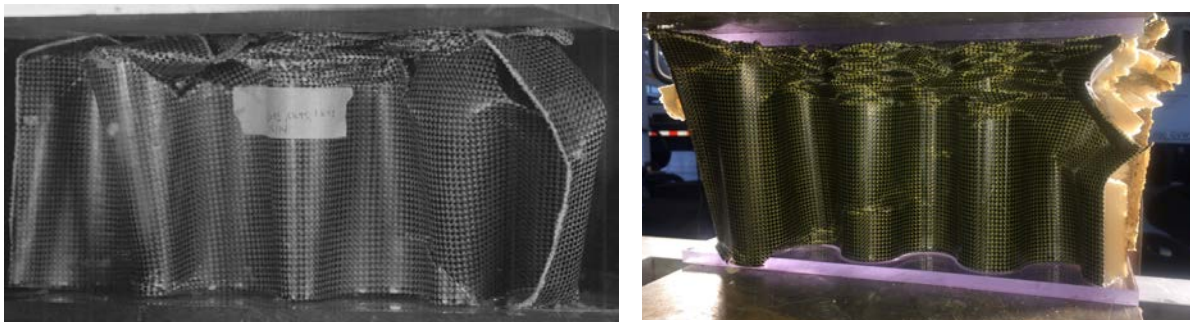

(a) Conusoid energy absorber. (b) Sinusoid energy absorber.

Figure 36. Post-test photographs of two NASA-developed composite energy absorbers.

Comparisons of predicted and experimental acceleration and displacement time histories of the drop mass are shown in Figures 37(a) and (b), respectively, for the conusoid energy absorber. The conusoid model over predicts the magnitude of the initial peak acceleration, 96-g compared with 61-g for the test. However, other than that anomaly, the level of agreement is good. The average acceleration calculated for the test is 28.0-g for pulse duration of 0.0- to 0.025-s, whereas the model average acceleration is 28.4-g for the same duration. The results of the conusoid component test indicate that the configuration of the energy absorber meets all of the design goals, including achieving a sustained average acceleration level of between 25-40-g. The comparison of vertical displacement time histories also exhibits good agreement, as shown in Figure 37(b). The maximum displacement of the test article is 2.9-in., providing a crush stroke of 38.7%. The maximum displacement of the model is 2.53-in., providing a crush stroke of 33.7%.

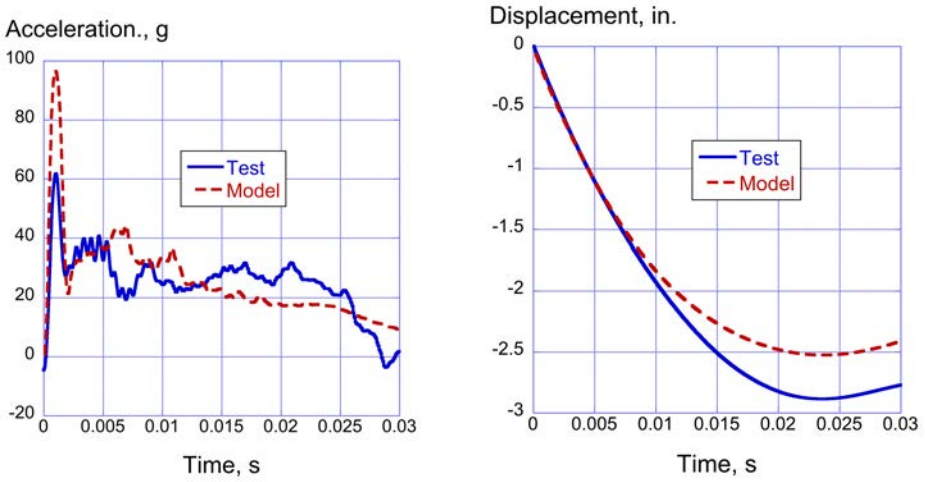

(a) Acceleration responses. (b) Displacement responses.

Figure 37. Acceleration and displacement comparisons for the conusoid component vertical drop test.

Test-analysis comparisons of time-history responses are plotted in Figure 38 for the sinusoid component crush test. These results demonstrate excellent test-analysis agreement. As can be seen in Figure 38(a), the acceleration response of the drop mass achieves an initial peak of 55-g, then drops to approximately 22-g, where it remains constant until the end of the pulse. The model mimics this response, even predicting the unloading response near the end of the pulse. The average acceleration calculated for the test is 21.8-g for pulse duration of 0.0- to 0.03-s, whereas the average acceleration of the predicted response is 22.9-g for the same duration. The experimental and analytical displacement responses, shown in Figure 38(b), exhibit maximum values of 4- and 3.8-in., respectively, which represents approximately 50% stroke. The average acceleration results for the sinusoid fall slightly below the required design goal of 25- to 40-g. However, the lower average crush acceleration for the sinusoid translates into a larger crush stroke than was seen for the conusoid.

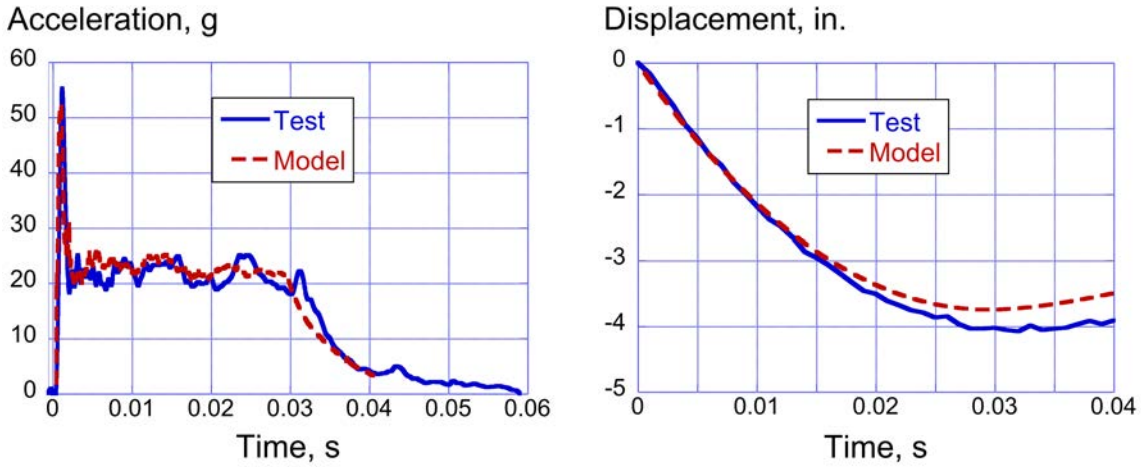

(a) Acceleration responses. (b) Displacement responses.

Figure 38. Test-analysis time history comparisons for the sinusoid component.

Following the TRACT 1 crash test, a portion of the forward cabin was separated from the remainder of the post-test specimen, as it was essentially undamaged during the TRACT 1 test. This barrel section was retrofitted with two of the energy absorbing concepts planned for TRACT 2, including the conusoid and the sinusoid foam sandwich designs. The original floor in the barrel section was removed and was replaced with a sheet of 0.5-in.-thick polycarbonate. The reason for this change was to enable viewing of the crushing response of the energy absorbers using high-speed cameras. The total weight of the fully loaded barrel section was 1,810-lb. The objectives of the barrel section test were to evaluate: (1) the performance of the two energy absorbers during a full-scale drop test prior to the TRACT 2 test, (2) the structural integrity of the retrofit, and (3) the strength of the polycarbonate floor.

Pre-test photographs of the barrel section test article are shown in Figures 39(a) and (b), highlighting front and rear views, respectively. Close-up photographs showing the conusoid and sinusoid foam sandwich energy absorbers that were retrofitted into the barrel section are shown in Figures 40(a) and (b), respectively. The conusoid subfloor was located at FS220. The floor of the fuselage section was

loaded with a 681-lb concentrated mass, which was centered about FS220 and located just above the conusoid energy absorber. The sinusoid energy absorber was located at FS190, in front of the conusoid. Both energy absorbers were painted white and vertical tick marks were added to aid in deformation tracking.

(a) Front view. (b) Rear view.

Figure 39. Front and rear view photographs of the CH-46E barrel section.

(a) Photograph of the conusoid energy absorber.

(b) Photograph of the sinusoid foam sandwich energy absorber.

Figure 40. Pre-test photographs of the conusoid and sinusoid energy absorbers, as retrofitted into the barrel section.

The floor of the fuselage section was loaded with a 320-lb concentrated mass on the right-hand side and a double seat with two 50th percentile male ATDs on the left-hand side, both centered about FS190 and located just above the sinusoid energy absorber. The seat was attached to the floor using standard seat tracks and the seated dummies were restrained using lap belts only. The combined

weight of the seat and dummies was 405-lb. This loading condition was intended to replicate the anticipated TRACT 2 configuration. The barrel section test was conducted by raising the test article to a height of 115.2-in. and releasing it to impact a concrete surface at 297.6-in/s. Data were collected at 25-kHz primarily from accelerometers located throughout the cabin and on the 320- and 681-lb masses.

A post-test photograph highlighting the crushing response of the conusoid energy absorber is shown in Figure 41. The original height of the conusoid was 8.31-in., as measured at the center of the subfloor, and the post-test height was 3.44-in., providing a crush stroke of 58%. As seen in Figure 41, the conusoid energy absorber displayed fracturing and delamination of the hybrid carbon-Kevlar® plies. Most of the damage was located in the center of the specimen, under the 681-lb mass.

Figure 41. Post-test photograph of the conusoid energy absorber.

Post-test photographs of the barrel section and the sinusoid energy absorber are highlighted in Figure 42. The original height of the sinusoid energy absorber was 8.75-in., as measured at the center of the subfloor, and the post-test height was 4.44-in., providing a crush stroke of 49.3%. As seen in Figure 42(b), the sinusoid foam sandwich energy absorber displayed crushing of the foam core, and fracturing of the face sheets starting from the bottom, curved edge. The sinusoid energy absorber in the barrel section did not exhibit the uniform folding pattern seen in the face sheets of the component specimen. As with the component crush tests, the barrel section drop test was simulated in LS-DYNA and the model demonstrated good prediction of the crush response of the energy absorbers [95].

(a) Post-test photograph of the barrel section.

(b) Post-test photograph highlighting the post-test crush response of the sinusoid.

Figure 42. Post-test photographs of the barrel section drop test.

A second CH-46E helicopter airframe (TRACT 2) was prepared for crash testing and loaded in a similar manner as the TRACT 1 test article [96]. The TRACT 2 aircraft was retrofitted with three different composite energy absorbing subfloor concepts. The shear panel at FS220 was replaced with a corrugated web energy absorber developed by the German DLR and the Australian ACS-CRC and fabricated of graphite fabric material [91, 92]. The shear panel at FS254 was replaced with the sinusoid foam sandwich energy absorber [94, 95] and the shear panel at FS286 was replaced with the conusoid energy absorber [93, 95]. A photograph depicting the retrofit of the sinusoid and conusoid energy absorbers into TRACT 2 is shown in Figure 43. The TRACT 2 full-scale crash test was conducted on October 1, 2014, and was performed for the same nominal impact velocity conditions and onto the same sand/clay surface as the TRACT 1 test.

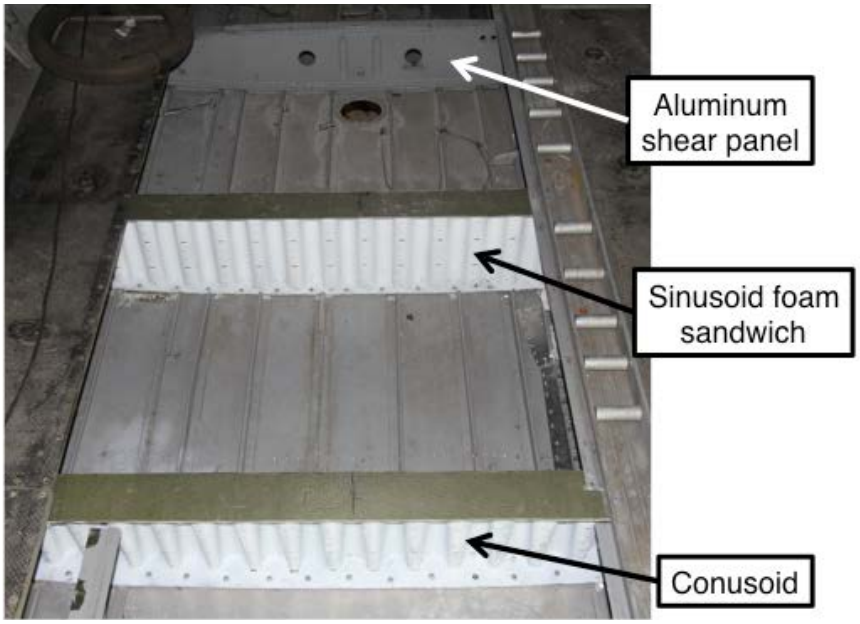

Figure 43. Photograph showing the retrofitted sinusoid and conusoid energy absorbers.

Unfortunately, results from the TRACT 2 full-scale crash test were complicated by several anomalies. Moist soil increased the coefficient of friction and reduced the stopping distance of the test article by half, compared with the TRACT 1 test. Due to excessive damage to the outer belly skin, the composite energy absorbers failed to crush and rotated globally as they became separated from the floor and outer skin under high shear loading. Another contributing factor was that modifications

were made to the floor structure, causing it to fail prematurely. Consequently, the results of this crash test are not included in this paper. Additional information is provided in Reference 95. Despite the shortfalls of the full-scale test, all three energy absorbers performed exceptionally well during their development phase, proving once again that composite structures can be designed to crush and to attenuate crash energy.

RECOMMENDATIONS FOR ROTORCRAFT CRASHWORTHINESS

Before concluding the paper, recommendations are suggested, such that the progress made to date in improved rotorcraft crashworthiness can be continued into the future. Please note that this list represents the author's opinion and does not represent official government policies or recommendations. The list is also not comprehensive. The recommendations are categorized using the same four specific topics discussed in the body of the paper: facilities and equipment for conducting crash testing, updated crash certification requirements, the application of crash modeling and simulation techniques, and rotorcraft structural design for improved crash performance focusing on the application of advanced composite materials.

Facilities and Equipment for Conducting Crash Testing

(1) The US Government should take the lead in maintaining state-of-the-art facilities for aircraft/rotorcraft crash testing and in upgrading equipment used to support crash testing as technology continues to advance.

(2) The second recommendation is to urge ATD manufacturers to development an ATD designed for vertical impact loading. While the market for these ATDs would be relatively small in comparison with the automotive industry, the need exists and it is important. Today, aircraft seats are being certified using ATDs that were designed and calibrated specifically for automotive crashes. Note that the US Army has invested in development of WIAMAN, which is an ATD designed for under-body blast [19]. This ATD has been specifically developed to overcome some of the deficiencies of existing ATDs, including providing accurate vertical loading along the spine. However, it has not been used in a full-scale crash test.

Updated Crash Certification Requirements

(3) As mentioned in this paper, accident studies were performed in the 1970's that were used in development of MIL-STD-1290A (AV) crash requirements. Army- and Navy-sponsored accident studies were performed in 2009 at the request of the US Congress. The long timespan between accident studies is unacceptable. It is recommended that the Army, Navy, Marine Corps, and the FAA with help from the National Transportation Safety Board perform routine decadal accident surveys on both military and civilian rotorcraft. This information would be used to assess the general level of crash performance of rotorcraft, to highlight specific issues that might need to be addressed, and to provide evidence that crash certification requirements are acceptable or need to be adjusted.

(4) It is recommended that whole-aircraft crash certification requirements be developed for civilian rotorcraft.

(5) It is recommended that the necessary steps be taken to build confidence in crash certification-by-analysis. This step is not intended to replace full-scale crash testing, but to limit the number of tests that may be necessary for certification.

Crash Modeling and Simulation Techniques

(6) It is recommended that accepted metrics for test-analysis correlation be developed. These metrics should be established industry-wide as a standard. Many methods exist that could be selected ranging from Sprague and Geers [97] to International Standards Organization 16250 [98] to CORelation of Analysis [99]. Perhaps, the recommended practice developed by the SAE for seat certification-by-analysis could be leveraged [100]. This document describes the use of modeling and simulation approaches for seat certification and provides the guidelines for calibrating analytical or virtual ATD models. As a suggestion, perhaps an American Helicopter Society International (AHSI) committee or subcommittee could be formed to review existing methods and make a recommendation, similar to the approach reported in Reference 101.

(7) It is recommended that an accurate ATD model be developed, such that the model reliably and accurately predicts the response of ATDs subjected to impact loading in the vertical or combined forward and vertical directions. Currently, ATD test responses obtained during a crash test are compared with ATD model predictions, to determine the likelihood of major injuries. In the near future, the impact responses could be used to assess soft tissue injuries using human occupant models such as the one developed by GHBMC [77, 78] or THUMS [79].

Rotorcraft Structural Design for Improved Crashworthiness

(8) This recommendation, which is to develop an energy absorbing subfloor concept optimized for multi-terrain impact, is especially challenging and may not be achievable. The difficulty of this task lies in the fact that dynamic responses of airframe structures subjected to impact onto rigid surfaces, soft soil, and water are very different. In the end, it may not be possible to fully optimize a crushable structure for all terrain impacts.

(9) This recommendation is to continue the systems approach to crash safety. The ACAP helicopters are prime examples that the systems approach works, without adding weight to the design. The rotorcraft community is urged to continue to utilize composite materials in helicopter design, where they make sense.

(10) Finally, in the future, novel rotorcraft configurations will be developed and these designs may require rethinking their crash behavior and their certification requirements. The rotorcraft community is urged to ensure that crash safety is considered, especially during early stages of design.

CONCLUDING REMARKS

This paper has documented advances in rotorcraft crashworthiness that have occurred over the past forty years. Trends are presented in several categories including: facilities and equipment for conducting crash testing, updated crash certification requirements, the application of crash modeling and simulation techniques, and rotorcraft structural design for improved crash performance focusing on the application of advanced composite materials. In the category of facilities and equipment for

crash testing, the Landing and Impact Research facility located at NASA Langley Research Center was described including recent facility upgrades. In addition, the LISA Aerospace Structures Impact Test Facility, located in Capua, Italy, and the Water Impact Research Facility, located at Yuma Proving Ground, were highlighted. Equipment for crash testing was presented including data acquisition systems, photogrammetry, Anthropomorphic Test Devices, and cameras. In crash certification, the evolution of crash criteria for military helicopters, starting with MIL-STD-1290A (AV) and ending with the Full Spectrum Crashworthiness criteria, was discussed. In the category of crash modeling and simulation, the early lumped-spring-mass kinematic code, KRASH, was described and an illustrative example of test-analysis comparison was presented for the Sikorsky Advanced Composite Airframe Program (ACAP) helicopter. Next, the state-of-the-art explicit, transient dynamic finite element code, LS-DYNA, was described. Data obtained from the full-scale crash test of a MD-500 helicopter were compared with analytical predictions from a system integrated LS-DYNA simulation. In addition, modeling of ATDs and multi-terrain impact simulations were highlighted. Finally, in the category of rotorcraft structural design, both the Bell and Sikorsky ACAP helicopters were described as excellent examples of the systems approach to crashworthiness. The Survivable Affordable Reparable Airframe Program Technology Validation Article was discussed, as well, as an example of a crashworthy composite structure. Finally, the development and evaluation of three composite energy absorbers were tracked from simple component tests to retrofit of subfloor sections into a CH-46E Sea Knight helicopter.

Prior to concluding the paper, the author provided a list of suggested recommendations, categorized under the same topic areas, such that the gains in rotorcraft crashworthiness that have been realized over the past four decades, can be continued into the future.

ACKOWLEDGEMENTS

I would especially like to thank Susan Gorton, who serves as the manager of the Revolutionary Vertical Lift Technology Project at NASA Langley, for nominating me for this award. Thank you, Susan, for your unwavering support of rotorcraft crashworthiness research at NASA! I would also like to thank the AHSI Awards Committee for selecting me for this award. I would like to thank my team members at NASA Langley for their support and hard work over many years in advancing the state-of-the-art in rotorcraft/aircraft crashworthiness. I would also like to acknowledge the members of the AHSI Crash Safety Technical Committee for being my colleagues and friends, and for supporting my nomination for this award. Finally, I acknowledge my family for their help and loving support over these many years. I want all of you to know that I am deeply honored and truly humbled by this award.

REFERENCES

1. Hurley T.R. and Vandenburg J.M., eds, “Small Airplane Crashworthiness Design Guide,” AGATE Report Number AGATE-WP3.4-034043-036, Simula Technical Report TR-98099, April 2002.

2. Couch M. and Lindell D., “Study on Rotorcraft Safety and Survivability,” Proceedings of the American Helicopter Society Forum 66, Phoenix, AZ, May 10-13, 2010.

3. Kent R., “Injury and Fatality Patterns in US Navy Rotary Wing Mishaps: A Descriptive Review of Class A and B Mishaps from 1985 to 2005,” Proceedings of the American Helicopter Society Forum 65, Grapevine, TX, May 27-29, 2009.

4. Labun L., “A Study of Rotary-Wing Crashes to Support New Crashworthiness Criteria,” Proceedings of the American Helicopter Society Forum 66, Phoenix, AZ, May 10-13, 2010.

5. https://ohsonline.com/articles/2017/02/14/faa-helicopter-accident-rates-decreasing.aspx, “FAA: Helicopter Accident Rates Dropping,” Feb 14, 2017.

6. Roskop, L., “US Rotorcraft Accident Data and Statistics,” Proceedings of the 2012 FAA/Industry Safety Forum, January 2012.

7. O'Bryan T. C. and Hewes D. E., "Operational Features of the Langley Lunar Landing Research Facility," NASA TN D-3828, February 1967.

8. O'Bryan T. C., "Flight Tests of a Manned Rocket-Powered Vehicle Utilizing the Langley Lunar Landing Research Facility," Proceedings of the AIAA Guidance and Control Specialists Conference, Seattle, Washington, August 15-17, 1966.

9. Vaughan V. L., Jr. and Alfaro-Bou E., "Impact Dynamics Research Facility for Full-Scale Aircraft Crash Testing," NASA TN D-8179, April 1976.

10. Jackson K. E., Boitnott R. L., Fasanella E. L., Jones L.E. and Lyle K. H., “A Summary of DOD-Sponsored Research Performed at NASA Langley's Impact Dynamics Research Facility (IDRF),” ***Journal of the American Helicopter Society***, Vol. 51, No.1, January 2006, pp 59-69.

11. Jackson K. E. and Fasanella E. L., “NASA Langley Research Center Impact Dynamics Research Facility Research Survey,” ***Journal of Aircraft***, Vol. 41, Number 3. May-June 2004, pp. 511-522.

12. Richards M. K. and Kelley E. A., “Development of a Full-Scale Crash Test Facility,” Proceedings of the Third International KRASH User’s Conference, Phoenix, AZ, January 8-10, 2001.

13. Jones L.E. and Fasanella E. L., “Instrumentation and Data Acquisition for Full-Scale Aircraft Crash Testing,” Proceedings of the 39th International Instrumentation Symposium, Instrument Society of America, Albuquerque, NM, May 2-6, 1993, pp. 903–913.

14. Littell J. D., “Large Field Digital Image Correlation used for Full-Scale Crash Testing: Methods and Results,” Proceedings of the Society of Experimental Mechanics International Digital Image Correlation Fall Conference, Philadelphia, PA, November 7-10, 2016.

15. Littell J. D., “Experimental Photogrammetric Techniques Used on Five Full-Scale Aircraft Crash Tests,” NASA TM-2016-219168, March 2016.

16. Annett M. S. and Littell J. D., “Evaluation of the Second Transport Rotorcraft Airframe Crash

Testbed (TRACT 2) Full Scale Crash Test," Proceedings of the 71st American Helicopter Society Forum and Technology Display, Virginia Beach, Virginia, May 5-7, 2015.

17. Smrcka J., "Dummies: Past and Present," http://www.humaneticsatd.com/about-us/dummy-history.

18. Backaitis S. H. and Mertz H. J., eds, ***Hybrid III: The First Human-Like Crash Test Dummy***, Society of Automotive Engineers (SAE) PT-44, 1994.

19. Baker W., Untaroiu C. and Chowdhury M., "Development of a Finite Element Model of the WIAMAN Lower Extremity to Investigate Under-Body Blast Loads," Proceedings of the 14th International LS-DYNA Users Conference, Dearborn, MI June 12-14, 2016.

20. Zimmerman R. E. and Merritt N. A., Aircraft Crash Survival Design Guide, Volumes I-5, Simula, Inc., Phoenix, Arizona; USAAVSCOM TR 89-D-22D, Aviation Applied Technology Directorate, US Army Aviation Research and Technology Activity (AVSCOM), Fort Eustis, Virginia, December 1989.

21. Military Standard, MIL-STD-1290A (AV), Light Fixed and Rotary-Wing Aircraft Crash Resistance, Department of Defense, Washington, DC, September 1988.

22. Anon., "Aeronautical Design Standard Rotary Wing Aircraft Crash Resistance," ADS-36, US Army Aviation Systems Command, St. Louis, MO, May 1987.

23. Bolukbasi A., Crocco J., Clarke C., Fasanella E., Jackson K., Keary P., Labun L., Mapes P., McEntire J., Pellettiere J., Pilati B., Rumph F., Schuck J., Schultz M., Smith M. and Vasquez D., "Full Spectrum Crashworthiness Criteria for Rotorcraft," RDECOM TR 12-D-12, December 2011.

24. Crocco J., "A Systems Approach to Crash Protection," Proceedings of the 68th American Helicopter Society Annual Forum, Fort Worth, TX, 2012.

25. Code of Federal Regulations, Title 14 Part 27 (14 CFR Part 27) Airworthiness Standards: Normal Category Rotorcraft, Federal Aviation Administration, Washington D.C.

26. Code of Federal Regulations, Title 14 Part 29 (14 CFR Part 29) Airworthiness Standards: Transport Category Rotorcraft, Federal Aviation Administration, Washington D.C.

27. Society of Automotive Engineering Aerospace Standard SAE AS8049 Rev A., "Performance Standard for Seats in Civil Rotorcraft, Transport Aircraft, and General Aviation Aircraft," 14 August 2015.

28. Bolukbasi A. O., "Crashworthy Design of Military and Civil Rotorcraft," Proceedings of the SAE Advances in Aviation Safety Conference, Daytona Beach, FL, 2000.

29. Coltman J. W., Bolukbasi A. O. and Laananen D. H., "Analysis of Rotorcraft Crash Dynamics for Development of Improved Crashworthiness Design Criteria," DOT/FAA/CT-85/11, 1985.

30. Code of Federal Regulations, Title 14 Part 23, (14 CFR Part 23), Airworthiness Standards: Normal, Utility, Acrobatic, and Commuter Category Airplanes, Federal Aviation Administration, Washington, D.C.

31. Code of Federal Regulations, Title 14 Part 25, (14 CFR Part 25) Airworthiness Standards: Transport Category Airplanes, Federal Aviation Administration, Washington, D.C.

32. Federal Register, Federal Aviation Administration, Aviation Rulemaking Advisory Committee, Transport Airplane and Engine Issues, Vol. 80, 2015.

33. Advisory Circular AC 20-146, "Methodology for Dynamic Seat Certification by Analysis for Use in Part 23, 25, 27, and 29 Airplanes and Rotorcraft," Federal Aviation Administration, 2003.

34. Jackson K. E., Fasanella E. L. and Lyle K. H., "Crash Qualification by Analysis – Are We There Yet," Proceedings of the American Helicopter Society Forum 62, Phoenix, AZ, May 9-11, 2006.

35. Gamon M., "General Aviation Airplane Structural Crashworthiness User's Manual Volume I Program KRASH Theory," Final Report FAA-RD-77-189, February 1978.

36. Gamon M., Wittlin G. and LaBarge B., "KRASH 85 User's Guide- Input/Output Format," Final Report DOT/FAA/CT-85/10, May 1985.

37. Hallquist J. O., "DYNA3D User's Manual: Nonlinear Dynamic Analysis of Structures in Three Dimensions," University of California, Lawrence Livermore Laboratory, Report UCID-19592, Rev. 4, April 1988.

38. Schreiber O., Schrauwen W., Devarco T., Shaw S. and Thomas D., "MSC Nastran Explicit Nonlinear (SOL 700) on Advanced SGI Architectures," SGI Tech Guide, http://sgi.com.

39. PAM-CRASH, "Virtual Prototyping Software and Solutions," ESI-Group, 2003.

40. Hallquist J. O., "LS-DYNA Keyword User's Manual," Volume I, Version 971, Livermore Software Technology Company, Livermore, CA, August 2006.

41. Hallquist J. O., "LS-DYNA Keyword User's Manual," Volume II Material Models, Version 971, Livermore Software Technology Company, Livermore, CA, August 2006.

42. Hallquist J. O., "LS-DYNA Theory Manual," Livermore Software Technology Company, Livermore, CA, March 2006.

43. Kay B. F. and Maass D., "Airframe Preliminary Design for an Advanced Composite Airframe Program, Basic Report," Volume 1, Parts 1-3, USAAVRADCOM-TR-80-D-35A, March 1982.

44. Carnell B. L. and Pramanik M., "ACAP Crashworthiness Analysis by KRASH," Proceedings of the AHS National Specialists' Meeting on Composite Structures, Philadelphia, PA, March 23-25, 1983.

45. Perschbacher J. P., Clarke C., Furnes K. and Carnell B., "Advanced Composite Airframe Program (ACAP) Militarization Test and Evaluation (MT&E) Volume V- Airframe Drop Test," USAATCOM TR 88-D-22E, March 1996.

46. Thomson D. T. and Clarke C. W., "Advanced Composite Airframe Program (ACAP) Militarization Test and Evaluation (MT&E) Volume I- Landing Gear Drop Test," USAAVSCOM TR-88-D-22A, August 1989.

47. Cronkhite J. D. and Mazza L. T., "Bell ACAP Full-Scale Aircraft Crash Test and KRASH Correlation," Proceedings of the 44th Annual Forum of the American Helicopter Society, Washington D.C., June 16-18, 1988.

48. Bark L.W. and Berry V. L., "Advanced Composite Airframe Program (ACAP) Militarization Test and Evaluation Program, Volume V Crash Test," USAAVSCOM TR 92-D-12E, August 1992.

49. Good D. E. and Mazza L. T., "Advanced Composite Airframe Program – Today's Technology," Proceedings of the 1987 NASA/Army Rotorcraft Technology Conference, Ames Research Center, Moffett Field, CA, March 17-19, 1987.

50. Kellas S., "Deployable Rigid System for Crash Energy Management," US Patent Nos. 6,755,453 on June 29, 2004; 6,976,729 on December 20, 2005; and 7,040,658 on May 9, 2006.

51. Kellas S., Jackson K. E. and Littell J. D., "Full Scale Crash Test of a MD-500 Helicopter with Deployable Energy Absorbers," Proceedings of the 66th AHS Forum, Phoenix, AZ, May 11-13, 2010.

52. Jackson K. E., "Predicting the Dynamic Crushing Response of a Composite Honeycomb Energy Absorber using a Solid-Element-Based Finite Element Model," Proceedings of the 11th International LS-DYNA Users Conference, Dearborn, MI, June 6-8, 2010.

53. Jackson K. E., Kellas S., Annett M. S., Littell J. and Polanco M. A., "Evaluation of an Externally Deployable Energy Absorber for Crash Applications," Proceedings of the International Crashworthiness Conference, Leesburg, VA, September 22-24, 2010.

54. Littell J. D., Jackson K. E. and Kellas S., "Crash Test of an MD-500 Helicopter with a Deployable Energy Absorber Concept," Proceedings of the International Crashworthiness Conference, Leesburg, VA, September 22-24, 2010.

55. Kellas S. and Jackson K. E., "Deployable System for Crash-Load Attenuation," ***Journal of the American Helicopter Society***, Vol. 55, No. 4, October 2010, pp. 042001-1 through 042001-14.

56. Jackson K.E., Fasanella E. L., and Polanco M. A., "Simulating the Response of a Composite Honeycomb Energy Absorber: Part 1. Dynamic Crushing of DEA Components and Multi-Terrain Impacts," 2012 ASCE Earth and Space Conference, Special Symposium on Ballistic Impact and Crashworthiness, Pasadena, CA, April 15-18, 2012.

57. Fasanella E. L., Annett M. S., Jackson K. E. and Polanco M. A., "Simulating the Response of a Composite Honeycomb Energy Absorber: Part 2. Full-Scale Impact Testing," Proceedings of the 2012 American Society of Civil Engineers (ASCE) Earth and Space Conference, Special Symposium

on Ballistic Impact and Crashworthiness, Pasadena, CA, April 15-18, 2012.

58. Jackson K.E., Fasanella E.L., Annett M.S. and Polanco M.A., "Material Model Evaluation of a Composite Honeycomb Energy Absorber," Proceedings of the 12th International LS-DYNA Users Conference, Dearborn, MI, June 3-5, 2012.

59. Jackson K.E., Kellas S., Horta L.G., Annett M.S., Polanco M.A., Littell J. D. and Fasanella E.L., "Experimental and Analytical Evaluation of a Composite Honeycomb Deployable Energy Absorber," NASA Technical Memorandum, NASA-TM-2011-217301, November 2011.

60. Annett M. S., Horta L. G., Jackson K. E., Polanco M. A. and Littell J. D., "Development, Calibration, and Validation of a System-Integrated Rotorcraft Finite Element Model for Impact Scenarios," NASA/TM-2012-217785, November 2012.

61. Guha S., Bhalsod D., and Krebs J., "LSTC Hybrid III Dummies, Positioning & Post-Processing, Dummy Version: LSTC.H3.103008_v1.0," LSTC Michigan, 30 October 2008.

62. Roberts J., Merkle A., Biermann P., Ward E., Carkhuff B., Cain R. and O'Connor J., "Computational and Experimental Models of the Human Torso for Non-Penetrating Ballistic Impact," ***Journal of Biomechanics***, Vol. 40, No. 1, 2007, pp. 125–136.

63. Horta L.G., Reaves M.C, Annett M.S. and Jackson K.E.: "Multi-Dimensional Calibration of Impact Models," ***Aeronautics and Astronautics***, edited by Max Mulder, ISBN 978-953-307-473-3, Chapter 15, pp. 441-457, September 2011.

64. Horta L. G., Jackson K. E. and Kellas S., "A Computational Approach for Model Update of an LS-DYNA Energy Absorbing Cell," ***Journal of the American Helicopter Society***, Vol. 55, No. 3, July 2010, pp. 032011-1 – 032011-8.

65. Polanco M. A. and Littell J. D., "Vertical Drop Testing and Simulation of Anthropomorphic Test Devices," Proceedings of the 67th American Helicopter Society Annual Forum, Virginia Beach, VA, May 3-5, 2011.

66. Littell J. D. and Annett M. S., "The Evaluation of a Test Device for Human Occupant Restraint (THOR) Under Vertical Loading Conditions: Part 1 – Experimental Setup and Results," Proceedings of the 69th American Helicopter Society Forum, Phoenix, AZ, May 21-23, 2013.

67. Fleck J. T., "Calspan Three-Dimensional Crash Victim Simulation Program," **Aircraft Crashworthiness**, Saczalski K., Singley III G. T., Pilkey W. D., and Huston R. L., eds. University of Virginia Press, Charlottesville, VA 1975, pp. 299-310.

68. Huston R. L., Passerello C. E., Harlow M.W. and Winget J. M., "The UCIN-3D Aircraft Occupant," **Aircraft Crashworthiness**, Saczalski K., Singley III G. T., Pilkey W. D., and Huston R. L., eds. University of Virginia Press, Charlottesville, VA 1975, pp. 311-324.

69. Karnes R. N., Toches J. L., and Twigg D. W., "PROMETHEUS – A Crash Victim Simulator," **Aircraft Crashworthiness**, Saczalski K., Singley III G. T., Pilkey W. D., and Huston R. L., eds. University of Virginia Press, Charlottesville, VA 1975, pp. 327-346.

70. Laananen D. H., "Simulation of an Aircraft Seat and Occupant in a Crash Environment," **Aircraft Crashworthiness**, Saczalski K., Singley III G. T., Pilkey W. D., and Huston R. L., eds. University of Virginia Press, Charlottesville, VA 1975, pp. 346-363.

71. Laananen D. H., "Development of a Scientific Basis for Analysis of Aircraft Seating Systems," Federal Aviation Administration, Report No. FAA-RD-74-130, US Department of Transportation, Washington D.C., January 1975.

72. Laananen D. H., "Human Body Simulations for Analysis of Aircraft Crash Survivability," Proceedings of the Fifth International Research Council on Biomechanics of Impacts, Birmingham, England, Sept. 9-11, 1980.

73. Laananen D. H., Neri L. M. and Nuckolls C. E., "Crashworthiness Analysis of Aircraft Seats Using Program SOM-LA," Society of Automotive Engineers (SAE) Paper 830747, 1984.

74. Bolukbasi A. O. "Computer Simulation of a Transport Aircraft Seat and Occupant(s) in a Crash Environment. Volume 2. Program SOM-TA (Seat/Occupant Simulation Model for Transport Aircraft), User's Manual," 1986.

75. Maltha J. and Wismans J., "MADYMO – Crash Victim Simulations: A Computerized Research and Design Tool," Proceedings of the Fifth International Research Council on Biomechanics of Impacts, Birmingham, England, Sept. 9-11, 1980.

76. Prasad P. and Chou C. C., "A Review of Mathematical Occupant Simulation Models," **Accidental Injury: Biomechanics and Prevention**, 2nd Edition, Nahum A. M., and Melvin J. W., eds, Springer, New York, pp. 121-186.

77. Schwartz D., "Development of a Computationally Efficient Full Human Body Finite Element Model," Master's Thesis, Biomedical Engineering Department, Wake Forest University, Winston-Salem, NC, May 2015.

78. Combest, J. and Wang J-T., "Status of the Global Human Body Models Consortium (GHBMC)," Proceedings of the SAE Government and Industry Meeting, Washington D.C., January 20-22, 2016.

79. Iwamoto M., Nakahira Y., Tamura A., Kimpara H., Watanabe I. and Miki K., "Development of Advanced Human Models in THUMS," Proceedings of the 6th European LS-DYNA Users Conference, pp. 47-56.

80. Baldwin, M., "Final Report – Recommendations for Injury Prevention in Civilian Rotorcraft Accidents," TR-00016, Simula Technologies, Inc., February 29, 2000.

81. Lu Z., Seifert M., Ho C-H., "Bird Impact Simulation of Polycarbonate Windshield Subject the Brittle Failure," Proceedings of the American Helicopter Society 71st Annual Forum, Virginia Beach, Virginia, May 5–7, 2015.

82. Jackson K. E. and Fuchs Y. T., " Comparison of ALE and SPH Simulations of Vertical Drop Tests of a Composite Fuselage Section into Water," Proceedings of the 10th International LS-DYNA Users Conference, Dearborn, MI, June 8-10, 2008.

83. Fasanella E.L., Lyle K.H., Jackson K.E., "Developing Soil Models for Dynamic Impact Simulations," Proceedings of the American Helicopter Society 65th Annual Forum, Grapevine, TX, May 27-29, 2009.

84. Thomas M.A., Chitty D.E., Gildea M.L., and T'Kindt C.M., "Constitutive Soil Properties for Unwashed Sand and Kennedy Space Center," NASA/Contractor Report, NASA/CR-2008-215334, July 2008.

85. Jackson K.E., Littell J.D., Fasanella E.L., Annett M.S., and Seal M.D., "Multi-Level Experimental and Analytical Evaluation of Two Composite Energy Absorbers," NASA Technical Memorandum, NASA/TM-2015-218772, July 2015.

86. Cartensen T. A., Townsend W. and Goodworth A., "Development and Validation of a Virtual Prototype Airframe Design as Part of the Survivable Affordable Repairable Airframe Program," Proceedings of the 64th American Helicopter Society Forum, Montreal, Canada, April 29-May 1, 2008.

87. Jackson, K. E. Fasanella, E. L., Boitnott, R. L. and Lyle, K. H., "Full-Scale Crash Test and Finite Element Simulation of a Composite Prototype Helicopter," NASA/TP-2003-212641, ARL-TR-2824, August 2003.

88. Jackson K. E., Littell J. D., Fasanella E. L., Seal M. D. and Annett M. S., "Impact Testing and Simulation of Composite Airframe Structures," NASA Technical Memorandum NASA TM-2014-218169, February 2014.

89. Jackson K. E., Littell J. D. and Fasanella E. L., "Simulating the Impact Response of Composite Airframe Components," Proceedings of the 13th LS-DYNA Users Conference, Dearborn, MI, June 3-5, 2014.

90. Fasanella E. L., Littell J. D., Jackson K. E. and Seal M. D., "Simulating the Impact Response of Full-Scale Composite Airframe Structures," Proceedings of the 13th LS-DYNA Users Conference, Dearborn, MI, June 3-5, 2014.

91. Kindervater C., Thomson R., Johnson A., David M., Joosten M., Mikulik Z., Mulcahy L., Veldman S., Gunnion A., Jackson A. and Dutton S., "Validation of Crashworthiness Simulation and Design Methods by Testing of a Scaled Composite Helicopter Frame Section," Proceedings of the American Helicopter Society 67th Annual Forum, Virginia Beach, VA, May 3-5, 2011.

92. Billac T., David M., Battley M., Allen T., Thomson R., Kindervater C., Das R., "Validation of

Numerical Methods for Multi-Terrain Impact Simulations of a Crashworthy Composite Helicopter Subfloor," Proceedings of the American Helicopter Society 70th Annual Forum, Montreal, Quebec, Canada, May 20-22, 2014.

93. Littell J. D., "The Development of a Conical Composite Energy Absorber for use in the Attenuation of Crash/Impact Loads," Proceedings of the American Society for Composites 29th Technical Conference, 16th US-Japan Conference on Composite Materials, September 8-10, University of California San Diego, La Jolla, CA.

94. Jackson K.E., Fasanella E.L., and Littell J.D., "Impact Testing and Simulation of a Sinusoid Foam Sandwich Energy Absorber," Proceedings of the American Society of Composites 30th Technical Conference, East Lansing, MI, September 28-30, 2015.

95. Jackson K.E., Littell J.D., Fasanella E.L., Annett M.S., and Seal M.D., "Multi-Level Experimental and Analytical Evaluation of Two Composite Energy Absorbers," NASA Technical Memorandum, NASA/TM-2015-218772, July 2015.

96. Annett M. S., Littell J. D., Jackson K. E., Bark L., DeWeese R. and McEntire B. J., "Evaluation of the First Transport Rotorcraft Airframe Crash Testbed (TRACT 1) Full-Scale Crash Test," NASA Technical Memorandum, NASA/TM-2014-218543, October 2014.

97. Sprague M.A. and Geers T. L., "Spectral Elements and Field Separation for an Acoustic Fluid Subject to Cavitation," ***Journal of Computational Physics***, Vol. 184, 2003, pp: 149-162.

98. Anon., "Road Vehicles - Objective Rating Metrics for Dynamic Systems," International Standards Organization Technical Report (ISO/TR) 16250, July 15, 2013.

99. Thunert C., CORA Release 3.6, User's Manual, 2012.

100. Society of Aerospace Engineers (SAE) Aerospace Recommended Practice (ARP) 5765A Analytical Methods for Aircraft Seat Design and Evaluation.

101. Schwer L.E., "Validation Metrics for Response Histories: Perspectives and Case Studies," ***Engineering with Computers***, Vol. 23, 2007, pp. 295-309.